Cement and Concrete Research 41 (2011) 679–695

Contents lists available at ScienceDirect

Cement and Concrete Research

journal homepage: http://ees.elsevier.com/CEMCON/default.asp

Thermodynamics and cement science

D. Damidot [a,b,*], B. Lothenbach [c], D. Herfort [d], F.P. Glasser [e]

[a] Université Lille Nord de France
[b] EM Douai, LGCgE-MPE-GCE, Douai, France
[c] Empa, Lab. Concrete & Construction Chemistry, Dübendorf, Switzerland
[d] Cementir Holding, Denmark
[e] Chemistry Department, University of Aberdeen, Aberdeen, UK

ARTICLE INFO

Article history:
Received 16 January 2011
Accepted 28 March 2011

Keywords:
Thermodynamic calculations (B)
Blended cements (D)
Fly ash (D)
$CaCO_3$ (D)
Solubility constant

ABSTRACT

Thermodynamics applied to cement science has proved to be very valuable. One of the most striking findings has been the extent to which the hydrate phases, with one conspicuous exception, achieve equilibrium. The important exception is the persistence of amorphous C–S–H which is metastable with respect to crystalline calcium silicate hydrates. Nevertheless C–S–H can be included in the scope of calculations. As a consequence, from comparison of calculation and experiment, it appears that kinetics is not necessarily an insuperable barrier to engineering the phase composition of a hydrated Portland cement. Also the sensitivity of the mineralogy of the AFm and AFt phase compositions to the presence of calcite and to temperature has been reported. This knowledge gives a powerful incentive to develop links between the mineralogy and engineering properties of hydrated cement paste and, of course, anticipates improvements in its performance leading to decreasing the environmental impacts of cement production.

Contents

* Corresponding author at: EM Douai, LGCgE-MPE-GCE, Douai, France.
E-mail address: damidot@ensm-douai.fr (D. Damidot).

0008-8846/$ – see front matter © 2011 Elsevier Ltd. All rights reserved.
doi:10.1016/j.cemconres.2011.03.018

1. Introduction

Thermodynamics is essential to our understanding of chemical reactions. With knowledge of just three so-called intensive variables, typically temperature, pressure and composition, we can predict if a reaction will take place and the final state once reaction is completed. The general laws governing thermodynamics are long known and were first applied to cement chemistry at the end of the 19th century by Le Chatelier [1] in order to demonstrate that cement hydration proceeds through the dissolution of solid cement clinker phases, leading initially to a supersaturated aqueous phase with respect to hydrates that subsequently precipitate from solution. These finally reach an equilibrium state with the remaining liquid phase contained in the porous network of the cement paste. Since then numerous studies have been reported in past ICCC's to experimentally or numerically define equilibrium conditions of hydrates and the composition of the aqueous phase in relation to the solids dissolved and precipitated [2–9].

In the meantime, thermodynamics have been applied to cement manufacturing. Indeed in the course of pyroprocessing, cement raw materials are reconstituted both chemically, by loss of structural water and carbon dioxide from the precursor minerals, and physically, as the complex but characteristic assemblage of minerals and microstructures develops in the course of processing. The tools used to quantify these reactions did not develop spontaneously but rely on applied thermodynamic approaches developed in several branches of science. For example, metallurgists have long sought to understand in a holistic way the complex relationships between alloy composition and thermal treatment, including the origin of microstructures and development of physical properties. In the natural sciences, petrologists have sought to understand these relationships amongst naturally-occurring systems mainly comprising oxides. In geology, clinkering corresponds closely to the formation of igneous rocks whilst cement hydration, with the important role of water, corresponds most closely to alteration and low-grade metamorphism.

Since the 1940s the pace of research in applied thermodynamics has gradually speeded up. Several factors are responsible for this acceleration, including advances in fundamental science and methodology. For example, significant advances have been made of our understanding of the role of highly disordered phases, including glasses, melts and gels and of their thermodynamic properties. Thus knowledge of the structure and composition of C–S–H gel structures was achieved first by chromatographic methods and, more recently and in greater depth, by NMR [10,11]. The structural models of C–S–H thereby developed supplement solubility measurements and enable a consistent thermodynamic approach to defining the C–S–H phase and its properties, despite its variable Ca/Si ratio and uncertain bound water contents. Other notable advances have occurred in developing thermodynamic treatments of concentrated aqueous solutions and in establishing links between kinetics and equilibrium.

Arguably, the greatest stimulus to the application of thermodynamics has arisen from the advent of electronic computational methods with which to undertake calculations. Inputs actually began in the pre-computer age: for example, the work of Hillert and colleagues [12] and of Kaufman and colleagues [13] on metals, and of Mchedlov-Petrossyan and colleagues on oxides, especially calcium aluminates and silicates [14]. However these pioneers had to work with hand computations, perhaps assisted by mechanical tabulators, and were additionally handicapped by access to inadequate databases. Thus, the importance of reliable databases was well-recognised and has resulted in gradual database improvements, particularly for refractory oxides and metals. Cements share some of these data, particularly for oxide substances such as CaO, MgO, Al_2O_3, SiO_2, etc. But significant advances in thermodynamic data for substances unique to cement have also been made, as will be described subsequently.

The development of computer-based codes for the minimisation of free energy began with, for example, the publication by the United States Geological Survey (USGS) of an open source code, and with the formation of the CALPHAD consortium [15]. Both are important starting points for modern methodologies. These codes work by minimisation of the free energy of a user-defined system and employ well-established mathematical shortcuts to facilitate convergence on a unique solution. In modern versions of these routines, the user also gains a number of freedoms: for example, the ability to specify composition or temperature, as well as the freedom to include, if desired, metastable states in the scope of calculation. This enables the metastable equilibrium between C–S–H and other, more stable, crystalline phases to be calculated. Different routines, some free, some commercial, all work in identical ways, although differing in user-friendliness, but will give essentially identical solutions using the same input data.

The following sections give examples of relevant applications to cement. Studies to date have generally shown that computer-based methods, coupled with adequate database support, can reliably predict the mineralogical composition of cement paste in terms of the relative content and composition of phases. Thus the metastable-equilibrium between C–S–H and other phases can in principle be predicted. One of the most interesting aspects of applying thermodynamics has been the discovery that the constitution of the minor phases, AFm and AFt, is very sensitive to temperature and the content of anions, especially carbonate, sulphate and hydroxide, and that the resulting phase distribution can change significantly, even over short ranges of temperatures, 0–40 °C [16,17]. Experimental verifications have shown that, in response to changing temperature, the equilibrium distribution of hydrate phases, amount and composition, does indeed shift rapidly, often within weeks or months, to reflect changing compositions and temperatures. Thus calculation and experiment are not competitive but instead support each other, with calculation enabling interpretation from limited sets of experimental data and identifying the key experiments that need to be performed to verify results of calculations. In addition, experiments are necessary to enrich and refine the accuracy of the database and to confirm the validity of predictions and identify kinetic barriers to equilibration, if any.

Finally, thermodynamics is also an invaluable tool assessing the durability of a cement paste in a given environment. Once equilibrium codes have been coupled with transport of matter, it becomes possible to predict the degradation rate of a cement paste and the evolution of its mineralogy in degraded zones [18]. When the timescale for reaction becomes too long to perform experiments, modelling becomes the only possible means of estimating the durability of cementitious materials in some very critical applications such as stabilisation and solidification of radioactive wastes.

This paper does not present a complete review of the work done on thermodynamic modelling applied to cement hydration over the past decades. It is, however, intended to demonstrate what can be achieved using thermodynamics in order to better understand and to model cement hydration both for academic and industrial studies; selected examples are cited. Moreover great care has been taken to present the actual limitations and also assist beginners in the field to avoid making common mistakes, as more and more people could be tempted to use thermodynamics owing to the availability of codes and databases. The relevance of using a thermodynamic approach rests largely on the need for precise numerical data on the thermodynamics of constituent phases. As a consequence, the first part of this paper mainly explains how to obtain the best possible thermodynamic data with respect to the solids involved in cement hydration. Then three examples of the application of thermodynamics applied to cement hydration are presented.

The calculation of saturation indexes from the composition of the aqueous phase recovered during hydration enables us to distinguish between the undersaturated phases which will dissolve and the supersaturated phases that may precipitate. The presentation of data as phase diagrams helps us to envisage the evolution of the stable phase assemblages of a given chemical system and its dependence on composition, temperature and pressure. Knowledge of the amount of the solids contained in the stable phase assemblages at complete hydration also enables us to evaluate the effect of reactive additions such as limestone or fly ash on phase compositions. Finally, with a few assumptions, these data can be linked to other material characterisation parameters such as porosity and the space-filling achieved by the solids.

2. Solubility data for cement hydrates

Thermodynamic equilibrium modelling is based on the knowledge of the thermodynamic data (e.g. solubility products and complex formation constants) of all the solids, aqueous and gaseous species that can form in the system. The quality of the results of thermodynamic modelling depends directly on the quality and the completeness of the underlying thermodynamic database. Nowadays geochemical software necessary for calculations is readily available but very often not directly useable for cement hydration mainly because thermodynamic data for relevant solids are lacking in the associated thermodynamic database. Thus the database has to be tailored by adding data for the missing solids and sometimes by also adding data for missing aqueous species *e.g.* complexes such as $Ca(OH)^+$. Three major sources can be used; the data can be determined experimentally, or found in the literature, or calculated from first principles or from analogous structures.

2.1. Available data

Thermodynamic data for complexes and solids generally present in geochemical systems, including gypsum and calcite, have been critically reviewed and reported in compilations (*e.g.* [19–24]). Specific thermodynamic data for other cementitious substances, such as the solubility products of ettringite or hydrogarnet, are usually not included in general databases but have been compiled separately in specific "cement databases". Cement-specific databases thus complement existing general databases but need to be harmonised with that particular general database.

The first compilation of thermodynamic data for cement minerals was published as early as 1965 by Babushkin et al. [25]. Several databases focusing on the solubility of cementitious materials based on the latest experimental data at the time of publication have appeared in the meantime, *e.g.* [26–34], including the two excellent datasets published in 1992 by Reardon [29] and by Bennet et al. [30]. Recently, two new specific cement databases have been published: the cemdata07 database [35–39] and the cement database by Blanc et al. [40,41]:

i) The cemdata07 database [35–39] is based on the Nagra/PSI geochemical database [24,42] and contains thermodynamic data for a number of cement phases (solubility product, Gibbs free energy, enthalpy, entropy, heat capacity and molar volume). Solubility data have been generally calculated following a critical review of the available experimental data and from additional experiments made either to obtain missing data or to verify existing data. Where necessary, additional solubility data were measured and compiled in a range of temperatures between 0 and 100 °C [35–37]. The resulting cemdata2007 database covers hydrates commonly encountered in Portland cement systems in the temperature range 0–100 °C, including C–S–H, hydrogarnet, hydrotalcite, AFm and AFt phases and their solid solutions. In 2010–2011, new data were reported for Friedel's and Kuzel's salt [43], for chromate-containing AFm and AFt phases [44,45], for hydrotalcite-like phases [46], for iron-containing calcium hemi- and monocarbonate hydrates [47] as well as for C–S–H [48]. Further publications of the solubility products of hydrotalcite-like solids [49], of iodide containing AFm phases [50] and of further Fe-containing AFm phases and hydrogarnet [51] are known to be in preparation.

In 2010 a cement database was published by Blanc et al. [40,41], which is consistent with the BRGM general database "Thermochimie6" and "Thermoddem" [52,53]. Blanc et al. [40,41] selected their data basically on the same measured dataset as cemdata07, but used a different selection procedure: all data with a charge imbalance of >5% (including all data where no measured pH values have been reported) were excluded. From the remaining data, the solubility measurements after the longest equilibration time were generally selected [41]. In most cases the differences between the Blanc et al. dataset and cemdata07 are relatively small with two important exceptions; the solubility constants selected for hydrogarnet and calcium monosulphaluminate hydrate, the latter commonly abbreviated as monosulphate (see Table 1).

Table 1 shows that due to the different selection procedures, the solubility of monosulphate is 0.6 log units higher whilst the solubility product of hydrogarnet is 0.6 log units lower in the database of Blanc et al. [40] compared to the cemdata07 database [35,36]. Both values are, however, well within the reported literature data range where reported solubility products for monosulphate range from −27.62 [28] to −29.43 [54–58], and for hydrogarnet, from −19.95 [28] to −23.13 [29,57]. However, even the relatively small differences between cemdata07 and the Blanc database lead to different calculated stable phase assemblages in hydrated Portland cement. For example, the cemdata07 database calculates C–S–H to coexist with solid portlandite, ettringite and (in the absence of calcite) monosulphate. However the database of Blanc et al. [41] predicts that hydrogarnet rather than monosulphate should be formed under the same conditions. This relatively small difference results in apparently different stable hydrate assemblages and underlines the importance of including sensitivity analysis in thermodynamic modelling studies. As the difference between the solubility products derived in the two databases is within experimental error, it is not a trivial task to assess which values are correct. However, there is evidence that even upon prolonged hydration up to 450 days monosulphate rather than hydrogarnet is stable in the presence of sulphate [36] and that hydrogarnet does not appear in hydrated Portland cements except at higher temperatures (>55 °C) [35,59].

The two sets of predictions are not necessarily contradictory as other parameters such as the existence of solid solutions amongst AFm phases and the size of the crystals can modify equilibrium

Table 1
Comparison of solubility products for ettringite, monosulphate and hydrogarnet at 25 °C and 1 bar.

Reaction			log K_{s0} Cemdata07 [35,36]	Blanc [41]
$Ca_6Al_2(SO_4)_3(OH)_{12}\cdot 26H_2O$	⇔	$6Ca^{2+} + 2AlO_2^- + 3SO_4^{2-} + 4OH^- + 30H_2O$	−44.90	−44.77
$Ca_4Al_2(SO_4)(OH)_{12}\cdot 6H_2O$	⇔	$4Ca^{2+} + 2AlO_2^- + SO_4^{2-} + 4OH^- + 10H_2O$	−29.26	−28.67
$Ca_3Al_2(OH)_{12}$	⇔	$3Ca^{2+} + 2AlO_2^- + 4OH^- + 4H_2O$	−20.84	−21.42

conditions. Indeed, the role of hydrogarnet in cement systems has puzzled scientists for decades. The C_4AH_x series of hydrates was reported to be metastable with respect to assemblages containing hydrogarnet. However hydrogarnet does not appear in Portland cements except perhaps in the course of high temperature (>55 °C) treatment. On the other hand, C_3A hydration leads to a rapid formation of hydrogarnet even at room temperature. The persistence of AFm has been variously explained and is often attributed to kinetic factors, namely the difficulty of nucleating hydrogarnet. However recent work has contributed two relevant discoveries (i) revision of the thermodynamic values of the AFm phases shows that C_4AH_{19} has a field of stability in the C–A–H system but its stability has an upper limit of ~8 °C, above which hydrogarnet becomes stable and (ii) the sulphate content of Portland cement forms AFm solid solutions with OH–AFm; partial replacement of OH by sulphate, as occurs spontaneously in Portland cement, stabilises AFm to progressively higher temperatures with respect to hydrogarnet. Thus in cement hydrated at ~25 °C, the non-appearance of hydrogarnet is expected and conforms to theoretical expectations [16]. This illustrates the importance of (i) using a reliable database and (ii) of using saturation indexes to search for other phase assemblages which might be stable and, given limits of data accuracy, consideration of both stable and persistent metastable assemblages especially when the calculated energetics are within limits of experimental error.

2.2. Determination of solubility data

2.2.1. Solubility data at standard conditions 25 °C, 1 bar

The thermodynamic properties of reaction or of a single species depend on temperature and pressure. Generally, tabulated thermodynamic data refer to the standard temperature and pressure of $T_0 = 298.15$ K (25 °C) and P = 1 bar (0.1 MPa), respectively. Solubility data might be (i) determined experimentally or (ii) calculated from basic thermodynamic properties of the constituents of the reaction, as illustrated below for the solubility product of gypsum.

i) experimental determination
The solubility of gypsum $CaSO_4 \cdot 2H_2O$ can be calculated directly from measured solubility data. Lilley and Briggs [60] determined the solubility of gypsum as 0.01518 mol/kg H_2O at 25 °C. To calculate the solubility, the formation of dissolved aqueous complexes needs also to be included. If gypsum is dissolved in H_2O, besides the aqueous Ca^{2+} and SO_4^{2-} also $CaSO_4^0$ will form: $\frac{\{CaSO_4^0\}}{\{Ca^{2+}\}\{SO_4^{2-}\}} = 10^{2.3}$. Combining that with the mass balance equations $m_{Catot} = m_{Ca^{2+}} + m_{CaSO4^\circ}$ and $m_{SO4\ tot} = m_{SO4}^{2-} + m_{CaSO4^\circ}$ one obtains, as $m_{Catot} = m_{SO4\ tot}$ and $m_{Ca^{2+}} = m_{SO4^{2-}}, m_{CaSO_4^0} = \frac{10^{2.3} m_{Ca^{2+}}^2 \gamma_{Ca^{2+}} \gamma_{SO_4^{2-}}}{\gamma_{CaSO_4^0}}$

where $\{i\} = \gamma_i * m_i$ is the activity, γ_i the activity coefficient and m_i the concentration in mol/kg H_2O. The activity coefficients γ_i can be calculated based on the ionic strength I using several published methods. For example, using the Davies equation: $\log \gamma = -Az^2\left(\frac{\sqrt{I}}{1+\sqrt{I}}\right) - 0.3I = -0.5z^2\left(\frac{\sqrt{I}}{1+\sqrt{I}}\right) - 0.3I$ one obtains $\gamma_{Ca}^{2+} = \gamma_{SO4}^{2-} = 0.42$ and $\gamma_{CaSO4^\circ} = 1.04$ at I = 0.06072 and thus:

$$m_{Ca_{tot}} = m_{Ca^{2+}} + \frac{10^{2.3} \times 0.42^2 \times m_{Ca^{2+}}^2}{1.04} = m_{Ca^{2+}} + 33.7 \times m_{Ca^{2+}}^2 = 0.01518.$$

Solving the quadratic equation we obtain $m_{Ca}^{2+} = 0.01106$ and $m_{CaSO4^\circ} = 0.00412$. As one third of the aqueous calcium and sulphate are bound in $CaSO_4^0$, one must recalculate the ionic strength and after a few iterations obtain $m_{Ca}^{2+} = 0.01047$ and $m_{CaSO4^\circ} = 0.0047$ and $\gamma_{Ca}^{2+} = \gamma_{SO4}^{2-} = 0.47$ and finally the following solubility constant, assuming an activity of 1 for H_2O:

$$\frac{\{CaSO_4 \cdot 2H_2O\}}{\{Ca^{2+}\}\{SO_4^{2-}\}\{H_2O\}^2} = \frac{1}{m_{Ca^{2+}}\ \gamma_{Ca^{2+}}\ m_{SO_4^{2-}} \gamma_{SO_4^{2-}} \{H_2O\}^2} = \frac{1}{0.01047^2 \times 0.47^2 \times 1^2} = 10^{4.61}.$$

If a still greater number of species are involved, geochemical software will usually have to be used to calculate the numerical values of the relevant constants. Applying a different model to calculate the activity corrections will lead to a slightly different solubility product, so the same activity correction model should be used consistently to derive solubility data and carry out calculations.

ii) calculation from basic thermodynamic properties
The Gibbs free energy of reaction is related to the Gibbs free energy of formation of the constituents according to:

$$\Delta_r G^{\circ\circ} = \sum_i \nu_i \Delta_f G^\circ = -RT\ ln\ K \quad (1)$$

where ν_i is the stoichiometric reaction coefficients, R = 8.31451 J/mol/K and T the temperature in K. Using the $\Delta_f G^\circ$ values of gypsum (−1797.238 kJ/mol), Ca^{2+} (−552.806 kJ/mol), SO_4^{2-} (−744.004 kJ/mol) and H_2O (−237.14 kJ/mol) as given in [30] results for $\{Ca^{2+}\}*\{SO_4^{2-}\}*\{H_2O\}^2 = CaSO_4\ 2H_2O$ (gypsum) in a Gibbs free energy of reaction of −26.148 kJ/mol. And according to

$$K_{S0} = e^{\frac{-\Delta_r G^\circ}{RT}} \quad (2)$$

$$\frac{\{CaSO_4 \cdot 2H_2O\}}{\{Ca^{2+}\}\{SO_4^{2-}\}\{H_2O\}^2} = 10^{4.58} \quad (3)$$

is obtained.

The result is in good agreement with the solubility data from the first method. However, data obtained from the first method is nevertheless preferred as it allows a more direct determination of gypsum solubility product than the second method and it can account for the effect of the size of the crystals as well as some impurities contained in the crystal structure.

2.2.2. Solubility at other temperatures

Different approaches may also be used to obtain thermodynamic data valid at different temperatures. Either the solubility can be measured at different temperatures and the solubility at other temperatures within this range interpolated or, alternatively, the temperature dependence can be measured or estimated from heat capacity, enthalpy or entropy data. Thus the Gibbs free energy and solubility as a function of temperature can be obtained. In any case, the data are only valid within the temperature range investigated.

2.2.2.1. Extrapolation based on measured solubility data. Measured solubility data for ettringite are available at different temperatures as shown in Fig. 1 for the reaction

$$Ca_6[Al(OH)_6]_2(SO_4)_3 \cdot 26H_2O \Leftrightarrow 6Ca^{2+} + 2Al(OH)_4^- + 3SO_4^{2-} + 4OH^- + 26H_2O.$$

The dependence of the solubility upon temperature can be expressed as:

$$\log K_T = A_0 + A_1 T + \frac{A_2}{T} + A_3\ lnT + \frac{A_4}{T^2} + A_5 T^2 + A_6\sqrt{T} \quad (4)$$

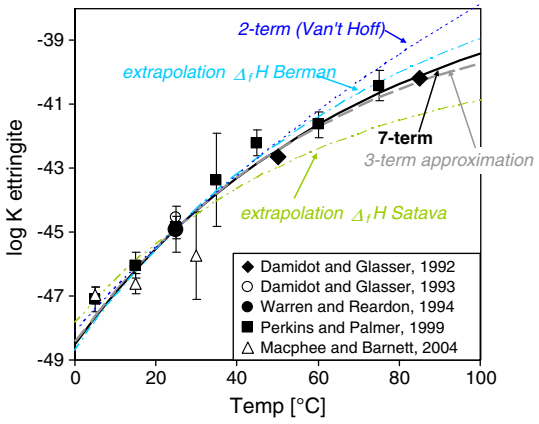

Fig. 1. Changes of ettringite solubility as a function of temperature compared to solubility products (points) calculated from measured concentrations from [54,57,64–66]. Lines correspond to the calculated course of reaction using different approximations (see text).

[61,62], where A_0, … A_6 are constants. If the entropy (S°), the enthalpy ($\Delta_f H°$) as well all the coefficients (a_0, a_1, …) of the heat capacity equation ($C°_p = a_0 + a_1 T + a_2 T^{-2} + a_3 T^{-0.5} + a_4 T^2$) of the species are available, the constants A_0, … A_6 can be calculated directly (see [63,64]), otherwise the constants can be fitted to experimental data, if available.

The value of $\Delta_r C_p^0$ in the temperature range 0–100 °C has little influence on the calculated log K value in Eq. (4), which makes it insensitive to the fitting procedure. Thus, the heat capacity of reaction is generally not fitted; instead, measured (or calculated) heat capacities of the solids are used [35,36,40,43,45,46]. For ettringite, Ederova and Satava [67] determined a heat capacity, Cp, of 2174.36 J/mol/K (= 1939 + 0.789 T; T: temperature in K).

Using the experimentally-determined solubility products at different temperatures shown in Fig. 1, an enthalpy of reaction $\Delta_r H°$ of 200.2 kJ/mol and an entropy $\Delta_r S°$ of −187.99 J/mol/K were fitted, corresponding to an enthalpy of formation $\Delta_f H° = -17{,}535$ kJ/mol and entropy S° of 1900 J/K/mol for ettringite. Only the enthalpy or the entropy values are fitted as they are interdependent via the Gibbs free energy $\Delta_f G°$: $\Delta G = \Delta H - T\Delta S$. This approach yields results corresponding to the curve labelled "7-term" (according to Eq. (4)) in Fig. 1.

The heat capacity of the reaction, $\Delta_r C_p^0$, is often only known at standard temperature and is thus assumed to be constant in the considered temperature range (for ettringite $\Delta_r Cp^0_{T_0}$ equals −1541 kJ/mol at 25 °C). If $\Delta_r Cp^0_{T_0}$ is constant ($\Delta_r Cp^0_{T_0} = \Delta_r Cp^0_T = -1541$), Eq. (4) can be reduced to the so called 3-term approximation of the temperature dependence:

$$\log K_T = A_0 + \frac{A_2}{T} + A_3 \ln T \tag{5}$$

$$A_0 = \frac{0.4343}{R} \cdot \left[\Delta_r S^0_{T_0} - \Delta_r Cp^0_{T_0}(1 + \ln T_0)\right] \tag{6}$$

$$A_2 = \frac{0.4343}{R} \cdot \left(\Delta_r H^0_{T_0} - \Delta_r Cp^0_{T_0} T_0\right) \tag{7}$$

$$A_3 = \frac{0.4343}{R} \cdot \Delta_r Cp^0_{T_0}. \tag{8}$$

The three term approximation is also suitable for non-isoelectric[1] reactions up to ~150 °C (see "3-term" in Fig. 1). Generally, the difference between the 7-term method and the 3-term approximation is small over the temperature interval 0–100 °C.

The two-term extrapolation (Van't Hoff equation)

$$\log K_T = A_0 + \frac{A_2}{T} = \frac{0.4343}{R}\left(\Delta_r S^0_{T_0} - \frac{\Delta_r H^0_{T_0}}{T}\right) \tag{9}$$

assumes that heat capacity of the reaction, $\Delta_r C_p^0 = 0$. Over a narrow temperature interval (±20 °C), good agreement is observed between the Van't Hoff equation and the 3-term approximation but at higher temperatures, ~100 °C, the difference increases (for example, up to 2 log units at 100 °C for ettringite). Thus the Van't Hoff equation is valid only for isoelectric or isocoulombic reactions (e.g. $Ca_6Al_2(SO_4)_3(OH)_{12}\cdot 26H_2O(s) + Fe_2O_3 \Leftrightarrow Ca_6Fe_2(SO_4)_3(OH)_{12}\cdot 26H_2O(s) + Al_2O_3$) but not for solubility reactions such as $Ca_6Al_2(SO_4)_3(OH)_{12}\cdot 26H_2O(s) \Leftrightarrow 6Ca^{2+} + 2Al(OH)_4^- + 3SO_4^{2-} + 4OH^- + 26H_2O$.

2.2.2.2. Extrapolation based on heat capacity, enthalpy or entropy data. If solubility data at different temperatures are not available, measured enthalpy and heat capacity data of the solid can be used to derive these data. As discussed above, Ederova and Satava [67] determined the heat capacity, Cp, of ettringite as 2174.36 J/mol/K. The enthalpy of formation $\Delta_f H°$ has been determined as −17,548 kJ/mol (−4194 kcal/mol) by Berman and Newman [68] and as −17,493 kJ/mol by Satava [67]. Using these data and the solubility determined at 25 °C, the apparent Gibbs free energy of formation $\Delta_a G°$ of ettringite between 0 and 100 °C can be calculated [61]:

$$\begin{aligned}\Delta_a G^o_T &= \Delta_f G^o_{T_0} - S^o_{T_0}(T - T_0) - \int_{T_0}^{T}\int_{T_0}^{T} \frac{C^o_p}{T} dT dT \\ &= \Delta_f G^o_{T_0} - S^o_{T_0}(T - T_0) - a_0\left(T \ln\frac{T}{T_0} - T + T_0\right) \\ &\quad - 0.5a_1(T - T_0)^2 - a_2\frac{(T - T_0)^2}{2T\cdot T_0^2} - a_3\frac{2\left(\sqrt{T} - \sqrt{T_0}\right)^2}{\sqrt{T_0}}\end{aligned} \tag{10}$$

where a_0, a_1, a_2, and a_3 are the empirical coefficients of the heat capacity equation $C°_p = a_0 + a_1 T + a_2 T^{-2} + a_3 T^{-0.5}$. The apparent Gibbs free energy of formation, $\Delta_a G°_{T,}$ refers to the free energies of the elements at 298 K. A more detailed description of the derivation of the dependence of the Gibbs free energy on temperature is given in [61,69,70]. The use of the enthalpy value measured by Berman and Newman [68], resulted in good agreement with the measured data, as indicated in Fig. 1, whilst the enthalpy data of Satava underestimated the solubility of ettringite especially at higher temperatures. If available, it is generally preferable to use measured solubility data at different temperatures.

In cases where neither measured enthalpy and heat capacity, nor solubility data at different temperatures are available, the entropy and heat capacity can be estimated using reference reactions based on structurally-similar solids with known S° and $C°_p$. If such reference reactions involve only solids and no "free" water, the change in heat capacity and the entropy are approximately zero [61,71,72]. For example, to estimate S° and $C°_p$ of thaumasite the following reference reaction has been used [72]: $3CaO\cdot Al_2O_3\cdot 3CaSO_4\cdot 32H_2O$(ettringite) + $2CaCO_3$(calcite) + $2SiO_2$(am) − $0.5CaSO_4\cdot 2H_2O$(gypsum) − $0.5CaSO_4$(anhydrite) − Al_2O_3(s) − $Ca(OH)_2$(portlandite) ⇔ $(CaSiO_3)_2(CaSO_4)_2(CaCO_3)_2\cdot 30H_2O$(thaumasite) resulting in entropy S° of 1900 + 2*93 + 2*41 − 0.5*194 − 0.5*107 − 51 − 83 ⇔ 1833). For thaumasite a good agreement between calculated solubility based on the estimated S° and $C°_p$ values [72] and measured solubility data at 5, 15 and 30 °C has been observed [73], (Fig. 2).

[1] An isoelectric reaction exhibits equal charges on both sides such as $Ca^{2+} + H_2O \leftrightarrow CaOH^+ + OH^-$, while an isocoulombic reaction is a reaction with identically charged species on either side (e.g. $Cl^- + H_2O \leftrightarrow HCl + OH^-$).

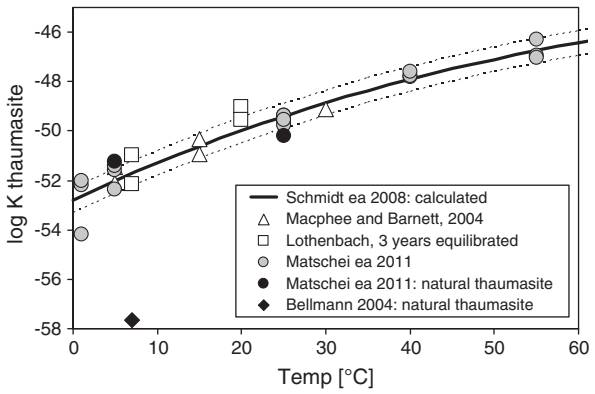

Fig. 2. Calculated solubility product of thaumasite as a function of temperature (from [39]) according to the reaction $(CaSiO_3)_2(CaSO_4)_2(CaCO_3)_2 \cdot 30H_2O(s) \Leftrightarrow 6Ca^{2+} + 2H_3SiO_4^- + 2SO_4^{2-} + 2CO_3^{2-} + 2OH^- + 26H_2O$ compared to solubility products derived from experimental data ([16,65,73] and new measurements) for synthesized and natural samples. Dotted lines indicate a 0.5 log unit variation of the calculated solubility product.

Further examples for the influence of temperature on the solubility of different solids important for cementitious materials are discussed in [35,36,40,41,43,47,64,66].

2.2.3. Effect of pressure and crystal size on solubility

The variation of Gibbs free energy varies with temperature, pressure and the composition of the phase, as stated by the Gibbs–Duhem relationship:

$$dG = -SdT + vdP + \sum_i \mu_i dn_i. \tag{11}$$

Thus the chemical potential and the solubility product also vary as a function of temperature, pressure as well as the composition of the phase. Temperature impacts can be well handled if care is taken, as described in the previous paragraph. Pressure is not often considered due to the lack of data but may be of importance in conditions such as oil well cementing, which corresponds to isobaric conditions (both liquid and solid at the same pressure). For example Seewald et al. [74] have noted that at both 1 and 500 bar, the solubility of portlandite decreases with increasing temperatures in the range from 100 to 350 °C and that portlandite solubility at 100 °C is 15 $mmol \cdot kg^{-1}$ at 500 bar compared with only 9.29 $mmol \cdot kg^{-1}$ at 1 bar. Thus pressure increases the solubility of portlandite. For a constant temperature, the following equations can be used to assess the effect of pressure when the equilibrium constant is known at atmospheric pressure (1 bar):

$$\left[\frac{\partial\left(\Delta G_r^0\right)}{\partial P}\right]_r = \Delta V_r^0 => \left[\frac{\partial\left(\ln K^0\right)}{\partial P}\right]_r = \frac{\Delta V_r^0}{RT}$$
$$\left[\frac{\partial^2\left(\ln K^0\right)}{\partial P^2}\right]_r = \frac{\partial\left(\Delta V_r^0\right)}{RT\,\partial P} \text{ thus } ln\left[\frac{K^p}{K^0}\right]_r = \frac{1}{RT}\int_0^p \Delta V_r^0 dP \tag{12}$$

where ΔV_r^0 is the volume change of the reaction and dP the change in pressure. If we consider the standard partial molar compressibility, $C_i^0 = \left(\frac{\partial V}{\partial P}\right)_T$, one can write :

$$\ln\left[\frac{K^p}{K^0}\right]_r = \frac{\Delta V_r^0 (P-1)}{RT} + \frac{\Delta C_i^0 (P-1)^2}{2RT}. \tag{13}$$

With respect to most of the hydrates of cementitious systems, the effect of pressure associated with temperature appears to be experimentally quite well understood for crystallised calcium silicate hydrates synthesised under hydrothermal conditions. A good summary of the phase equilibrium for the $CaO–Al_2O_3–SiO_2–H_2O$ system at 200 °C has been recently reported [75].

All the thermodynamic calculations reported in this paper have been obtained in an excess of water and thus only water-saturated solid phases occur. However, cement paste is generally unsaturated and, as a consequence, the liquid phase may be under a negative pressure whilst the solid is still at atmospheric pressure (anisobaric conditions). This is expected to markedly change solubilities, especially for low relative humidity where there is meniscus formation in very small pores — an occurrence not often considered in modelling of cement paste. However, this state has been recently modelled for unsaturated soils using a physicochemical model of capillary water in which the chemical potential of the capillary water is explicitly calculated, as well as its consequences to the thermodynamics of the capillary water–mineral–soil atmosphere system [76–78]. The effect of capillarity on the aqueous speciation and the solubility of minerals and gases in capillary solutions have been defined in general terms [79]. For example, under negative pressure conditions, the equilibrium constant of gypsum decreases leading to solubility that decreases from 14.4 $mmol \cdot kgw^{-1}$ at P = 0.1 MPa (atmospheric pressure) to 6.13 $mmol \cdot kgw^{-1}$ at P = −100 MPa [78]. Thus the effect of negative pressure may have to be considered to better simulate the thermodynamics of unsaturated cement pastes.

Returning to the Gibbs–Duhem equation, the term related to the composition of a phase, such as the molar fractions n_i of its components, is generally not taken into account in solubility calculations. However it is known that the solubility depends on crystal size: for spherical crystals, the solubility of smaller crystal sizes, the notion of "phase", as defined by thermodynamics, is not so obvious and one has to consider the effect of the surface and its curvature in addition to the volume. The following simplified relationship can be used as a first approximation to calculate the solubility for spherical particle having a radius r where r is <50 nm:

$$C_S(r) = C_S\, exp\frac{2\gamma \cdot V}{RTr} \tag{14}$$

where C_s is the solubility for large crystals and γ is the solid particle surface tension, V the molar volume of the solid, and R the universal gas constant.

When determining solubility experimentally, it is important to check the size of the crystals, knowing that the crystal size increases with time in order to reach more stable equilibrium conditions, *i.e.*, lower solubility. This growth process, so-called Ostwald ripening, operates for cement hydration with coarsening of the microstructure, especially at long ages.

2.3. Maintenance of the thermodynamic database

As reported above, several authors propose their own cement thermodynamic databases tailored for use with a specific geochemical code and caution must be taken when trying to transfer these data to a different thermodynamic database, especially if the geochemical code differs. Indeed, even if a solubility product is a constant, its value differs slightly depending on the geochemical code used. This is partly due to differences in the method used to estimate the activity of aqueous species but also to the nature of the aqueous species included in the thermodynamic database; these factors are often not explicit. A simple demonstration compares the dissolution of portlandite ($Ca(OH)_2$):

$$Ca(OH)_2 \Leftrightarrow Ca^{2+} + 2OH^-.$$

The solubility product is defined by the following equation considering that the activity of water is equal to 1:

$$K_{CH} = (Ca^{2+}) \cdot (OH^{-})^2.$$

If we consider two databases in which the first database (db1) contains Ca^{2+} and $CaOH^{+}$ as the Ca-containing aqueous species whilst the second database (db2) contains only Ca^{2+}, the value of log K for portlandite at 25 °C differs slightly between the two databases; $\log K_{CHdb1} = 22.815$ and $\log K_{CHdb2} = 23.07$, respectively. However, in practice, the use of K_{CHdb1} associated with the second database or of K_{CHdb2} with the first database leads to very poor results concerning the calculation of the solubility of portlandite (Table 2).

Another possible source of error arises if the value of the solubility product is given without defining a chemical equation for the dissolution of the solid. Indeed, the master aqueous species used to code the chemical equations may differ between codes; different master species lead to different values of the solubility product for the same solid. Consider the case of ettringite. The chemical equation relative to ettringite dissolution can be written as:

$$3CaO \cdot Al_2O_3 \cdot 3CaSO_4 \cdot 32H_2O \Leftrightarrow 6Ca^{2+} + 2Al(OH)_4^- + 3SO_4^{2-} + 4OH^- + 26H_2O.$$

As a consequence, its solubility product would be defined by the following equation assuming that the activity of water is equal to 1:

$$K_{sp1} = (Ca^{2+})^6 \cdot (Al(OH)_4^-)^2 \cdot (SO_4^{2-})^3 \cdot (OH^-)^4.$$

However if Al^{3+} and H^{+} are instead used as master species, the defining chemical equation for ettringite dissolution would be written as:

$$3CaO \cdot Al_2O_3 \cdot 3CaSO_4 \cdot 32H_2O \Leftrightarrow 6Ca^{2+} + 2Al^{3+} + 3SO_4^{2-} - 12H^+ + 38H_2O$$

and the solubility product as:

$$K_{sp2} = (Ca^{2+})^6 \cdot (Al^{3+})^2 \cdot (SO_4^{2-})^3 \cdot (H^+)^{-12}.$$

It is however possible to relate K_{sp1} and K_{sp2} using the two following equations concerning the aqueous species:

- for water dissociation;

$$Kw = \left(H^+\right) \cdot (OH^-)$$

- and $Al(OH)_4^-$ dissociation;

$$Kz = \frac{(Al(OH)_4^-)}{(Al^{3+}) \cdot (H^+)^{-4}}.$$

Thus we can write:

$$Ksp2 = \frac{\left(Ca^{2+}\right)^6 \cdot (Al(OH)_4^-)^2 \cdot \left(SO_4^{2-}\right)^3 \cdot (OH^-)^4}{Kz^2 \cdot Kw^4} = \frac{Ksp1}{Kz^2 \cdot Kw^4}.$$

As a consequence:

$$\log K_{sp2} = \log K_{sp1} - 2.\log Kz - 4.\log Kw.$$

Table 2
Solubility of portlandite at 25 °C in mM depending on the database used and the value of the solubility product of portlandite. The expected value is 22.02 mM.

	Log K_{CHdb1}	Log K_{CHdb2}
Solubility with database 1 (mM)	22.02	28.67
Solubility with database 2 (mM)	17.51	22.02

The composition of the aqueous phase in equilibrium with the solid should be given in order to enable the calculation of a well-defined solubility product; in this case the procedure to add the solid to the database would be identical to the situation where the solubility is determined experimentally as reported previously. Consequently if a numerical value of the solubility product is only given this could be ambiguous.

On the other hand, the accuracy of the thermodynamic database can be easily assessed from the calculation of the aqueous phase composition of known invariant points of selected chemical systems at given T and P and comparison with experiment. The use of invariant points of complex systems such as the $CaO–Al_2O_3–SiO_2–CaSO_4–CaCO_3–H_2O$ system [80] is thus an efficient method to test the accuracy of the database, assuming experiments actually attain equilibrium. This test can be applied automatically using specific codes in order to build the input files for the geochemical software and also to analyse the results. As a consequence, a specific method can be developed to verify the database each time it is modified. This methodology can be used to compare existing geochemical codes associated with a specific thermodynamic database. From this point of view one notes a general lack of thermodynamic database benchmarking in the literature and the absence of international validation of the results given by geochemical codes associated with specific thermodynamic databases.

Finally, the minerals contained in the clinker of the cements are often not found in thermodynamic databases because an experimental determination of their solubility is generally not possible due to the precipitation of hydrates of uncertain composition and crystallinity. However solubility constants may be estimated using the Gibbs free energy of reaction as reported before. The impact of impurities, leading to different crystallographic polymorphs or significant concentrations of chemically-induced crystal defects could best be assessed by experiment, or by molecular modelling or a combination. Moreover the application of thermodynamics to the first stages of hydration of clinker phases [81] has shown anomalies. For example, the expected solubility of tricalcium silicate is very high when calculated using the Gibbs free energy of reaction but is found experimentally to be quite low. Of course, it is long known that the dissolution is apparently incongruent and restricted due to both the formation of an intermediate phase slightly differing in composition from tricalcium silicate on its surface and precipitation of C–S–H [81]. It has been hypothesised that this intermediate phase very rapidly covers the surfaces of tricalcium silicate and thus controls the aqueous phase composition. As a consequence the solubility of the intermediate phase should be entered in the thermodynamic database in order to better model hydration of tricalcium silicate.

3. Use of the thermodynamic approach

3.1. Saturation indexes

When the aqueous phase composition is determined during cement hydration, by extraction of the aqueous phase in contact with cement paste, or sampling using a stirred cement suspension, some important insights of the mechanism of hydration can be obtained by calculation of the saturation index of the solids in contact with the aqueous phase. The saturation index, β, is defined for a solid A in contact with the aqueous phase by considering the variation of Gibbs free energy:

$$A_s \rightarrow mM + nN + \ldots$$

$$\Delta G_r = \Delta G_r^0 + RT \ln\left(\frac{a_M^m a_N^n \ldots}{a_{As}}\right).$$

At equilibrium $\Delta G_r^0 = -RT \ln K$, thus

$$\Delta G_r = RT \ln\frac{IAP}{K} = RT \ln \beta \quad (15)$$

where the ion activity product, IAP, refers to the product calculated from the measured aqueous concentrations and K to the respective solubility product.

If, for a given solid, $\beta<1$, the aqueous phase is undersaturated with respect to the solid. The solid will then dissolve in order to reach equilibrium *i.e.*, an aqueous phase composition corresponding to its solubility will be attained. On the other hand, if the solid is not present, it will not precipitate.

If $\beta>1$ the aqueous phase is supersaturated with respect to that solid. If the solid is present, it is stable but a larger quantity of the solid will be formed by precipitation until equilibrium with the aqueous phase is reached (an aqueous phase composition corresponding to its solubility will be attained). On the other hand, if the solid is not present, it should precipitate, perhaps after an induction period whose duration will depend on several factors, β being one of them: β increasingly >1 progressively reduces the duration of the induction period. If the aqueous phase is supersaturated with respect to several solids, the first to precipitate will generally have the shortest induction period so these solids may precipitate at different times.

As a consequence, the knowledge of saturation indexes during the course of cement hydration enables us to calculate which solids dissolve and which may precipitate. The data are thus complementary to the mineralogical determination of the solids formed during the course of hydration. Also, the determination of β corresponding to extremely short induction periods induces a quasi-immediate precipitation of a given solid, termed β_c, and it is very important to understand the mechanism of early cement hydration. The specific conditions leading to immediate precipitation that relies on kinetics, can however be calculated using a biased thermodynamic approach by considering a hypothetical critically supersaturated solid having an apparent solubility constant that varies with the aqueous phase composition:

$$\mathrm{Ln}\,K_{\text{critically supersaturared solid}}(\text{parameters}) = \mathrm{Ln}\,K_{\text{solid}} + \mathrm{Ln}\,\beta\,(\text{parameters}). \tag{16}$$

The relation of Ln β (parameters) to precipitation can only be derived from experiment. For example, the critically supersaturated domain of ettringite can be determined from thermodynamic calculation by considering a critically supersaturated ettringite having a variable value of its ion activity product, β_E, considered as an apparent solubility product and calculated using the following equation [82]:

$$\mathrm{Ln}\,\beta_E([\mathrm{Al}],[\mathrm{SO_4}]) = 7.74635 + 4.331082\ln([\mathrm{Al}]) + 2.205813\ln([\mathrm{SO_4}]).$$

As an example, the critically supersaturated domain of C_2AH_8 has been used to explain the difference between the hydration of $C_{12}A_7$ and C_3A at room temperature [83]. However when gypsum is added to C_3A, C_2AH_8 is no longer the first hydrate to form. Instead ettringite forms even though these two hydrates both become rapidly supersaturated: indeed the critically supersaturated domain of ettringite is reached before that of C_2AH_8 [82].

3.2. Phase diagrams

Knowledge of the phase diagram of a chemical system relevant to the chemistry of cement hydration is very helpful to correlate experimental results. Firstly, it enables us to determine the phase assemblages of minerals that are stable as a function of the evolution of some parameters, such as the concentration of a component, or changing temperature. The great strength of phase diagram is that the stable phase assemblages of a given chemical system remain stable in chemical systems of greater complexity. So it is possible to explore step by step chemical systems of increasing complexity. Secondly, from knowledge of the phase diagram, it is possible to determine if a phase assemblage found experimentally is stable or not. A weakness of phase diagrams is their limited dimensionality: it becomes progressively more difficult to represent systems with more than three components without simplifications. However phase diagrams of multicomponent systems and calculation are complimentary.

In actual applications we need to distinguish between open and closed systems. Closed systems are, as the term implies, closed to transfer of mass in and out of the defined system — some part of the material universe that can be isolated for separate study. Energy is, however, allowed to transport beyond the system boundary. Open systems, on the other hand, are open to transport of energy as well as to a limited and defined extent, of mass. The system concept is almost universally employed in the design of experiments on cements, even if not specifically identified. For example, the process of cement carbonation by atmospheric CO_2 involved open system behaviour but the system is nominally open only to gain of carbon dioxide and loss of water. Thus, in determining the resistance of cement to aggressive agents involving loss or gain of matter, the processes are first identified and studied one at a time before attempting to couple processes.

Not surprisingly, the fastest progress has been made in the thermodynamic analysis of closed or nearly closed systems, *i.e.*, where mass either remains constant in the course of reaction, or changes in a well-defined way. An example is in delayed ettringite formation where sulphate remains constant but is redistributed amongst phases as a consequence of changing temperature. Open systems present greater challenges not only to theoreticians but also to experimentalists, as it is necessary to define mass fluxes and transport kinetics.

By the start of the 20th century, efforts were being made to calculate phase equilibria. For example, van Laar [84] devised a series of algebraic equations which, from knowledge of the thermodynamic properties of the substances involved, could be used to predict binary (two component) systems. The method was not immediately successful mainly because of lack of knowledge concerning the number of phases in “unknown” systems, of phase compositions, of the thermodynamic properties of the solids and of concentrated aqueous solutions.

Numerous experimental works were thus done to determine the equilibrium conditions of hydrates and construct phase diagrams [85–102]. However once a phase diagram contains more than ~10 stable phases and 4 components other than water, the phase diagram becomes very complex and is difficult to explore experimentally. Similar difficulties are found for phase diagrams relative to high temperature processes such as those involved in the clinkering of cement. Thus the most complex cement-related systems were quinary, studied by Jones in 1944 [90,91]. On the other hand, thermodynamics enable rapid calculation of the equilibrium state of a given chemical system at given T and P. Their calculation became practical during the early 1980s thanks to the occurrence of computers and codes devoted to geochemistry. Nowadays these codes such as PHREEQC are readily available although the same cautions have to be raised about thermodynamic databases associated to these codes as were discussed previously.

The reliability of constructing a phase diagram for a given chemical system depends on two steps: the first is to define all the stable invariant points and the second, to deduce from the stable invariant points all the stable phase assemblages having fewer phases than the phase assemblages corresponding to the stable invariant points.

In order to determine all the stable invariant points for a chemical system relevant to cement hydration, the phase rule is applied to define the maximum number of solids that are in equilibrium with the aqueous phase at invariant points (no degrees of freedom). For example, in a system having C components, one of them being water, it is necessary to have C-1 solids in equilibrium with the aqueous phase at T and P fixed to define an invariant point. As a consequence, if Y solids exist containing one or several of the C constituents of the

chemical system, one can determine all the phase assemblages of C-1 solids. The number of phase assemblages of C-1 solids corresponds to the linear combinations for C-1 solids amongst Y. Once all the combinations of C-1 solids have been defined, one can calculate the aqueous phase in equilibrium with these solids with geochemical codes and thus determine if the phase assemblage is stable: this will be assured if no other solids are supersaturated with respect to the aqueous phase. Of course additional codes can be specifically developed to make the input files and to check the output file automatically and thus speed the calculation process. Once again, it has to be recalled that the accuracy of the results will depend on the accuracy of the thermodynamic database and on the fact that all stable solids have been included.

The number of combinations can also be reduced by removing the combinations of solids that are not stable from the knowledge of chemical systems having less than the C constituents. For example, if the combination of AH_3 and CAH_{10} is not a stable solid assemblage in the $CaO–Al_2O_3–H_2O$ system, no combinations of these phases will be stable in the $CaO–Al_2O_3–CaSO_4–H_2O$ system. This method very efficiently reduces the number of combinations that have to be calculated. For example, if we consider the $CaO–Al_2O_3–CaSO_4–CaCO_3–CaCl_2–H_2O$ system at T = 25 °C and P = 1 bar, the number of combinations of 5 solids to be calculated reduces from 792 to 19 if the metastable assemblages are not considered [103].

From the knowledge of the stable invariant points, it is therefore possible to draw some graphical representations of the phase diagram, totally or partly, depending on the number of components. These representations are helpful to visualise the evolution of the system with a selected parameter, such as a change in the concentration of one component. Simplified phase diagrams can be drawn by just linking the invariant points with straight lines. Fig. 3 presents the differences between the "real" drawing of the phase diagram of the $CaO–Al_2O_3–CaSO_4–H_2O$ system at T = 25 °C and P = 1 bar (right) and the simplified phase diagram, plotted by joining the relevant invariant points with straight lines (left). The complete conditions of the calculation of the phase diagram have to be stated: for example, acidic conditions are not represented in Fig. 3 because all solid combinations self-generate an aqueous pH > 7. Also, the numerical values of the solubility products used in this example did not admit monosulphate as a stable phase.

It is also of interest to deduce from the stable invariant points all the stable phase assemblages having fewer solids than the phase assemblages corresponding to stable invariant points. This is quite straightforward for chemical systems having less than 5 components. For example, let us consider an invariant point ABCD. The phase assemblages and the phases derived from this invariant point are: ABC, ACD, BCD, AB, AC, BC, AD, CD, A, B, C and D. For more complex chemical systems, it is easier to use a code that can provide a list of results and also results of an automatic search for stable phase assemblages. For example, the phase diagram of the $CaO–Al_2O_3–SiO_2–CaSO_4–CaCO_3–H_2O$ system at 25 °C and 1 bar pressure consists of 15 solid phases defining 331 stable phase assemblages in equilibrium with the aqueous phase amongst with 30 invariant points [80]. This phase diagram is the most complex which has been completely calculated for cementitious systems, yet one must be aware that, because of the influence of minor components on phase formation, major portions of the $CaO–Al_2O_3–SiO_2–Fe_2O_3–MgO–CaSO_4–CaCO_3–Na_2O–K_2O–H_2O$ system have to be known to obtain a complete overview of the different phase assemblages that may form during cement hydration. Thus considerable challenges remain.

Most of the calculations consider that water is in excess and that the activity of water is 1 or close to 1. This is true during early hydration, when water is in excess and the total of dissolved matter is low; however at later ages, when the porous network of the cement paste is not completely filled with water and the remaining "water" contains much dissolved alkali, one has to consider the impact of changes to the chemical potential of "water". A first attempt has been made to consider the reduced activity of water in the $CaO–Al_2O_3–CaSO_4–H_2O$ system at T = 25 °C and P = 1 bar [104] but without considering the possible effect of the negative pressure of the pore fluid solution. It shows that monosulphate could become a stable phase at relative humidity less than 66%. Nevertheless, this threshold value of relative humidity has to be taken with caution as the calculations did not take into account the loss of water molecules from other hydrates, especially ettringite, as functions of relative humidity.

3.3. Stable hydrate assemblages

Thermodynamic modelling can be used to calculate the stable phase assemblage after long hydration times assuming partial or complete hydration of the starting materials. However changes in the overall chemical composition of a system or a different temperature affect the amount as well as the identity of the solid phases. These calculations can be used to predict the changes in total volume and in porosity, in the post-hardened state. *Mass balance calculations* based on the chemical composition of the unhydrated cement are the easiest way to calculate the phase composition of a hydrated cement [105,106]. Such calculations can be carried out with a calculator, but with the disadvantage that the phase assemblage has to be known beforehand. For less well-characterised systems, *thermodynamic modelling* enables us to predict the nature of the hydrates as well as the composition of the aqueous phase. Thermodynamic calculations permit parametric variations and thus the systematic study of the

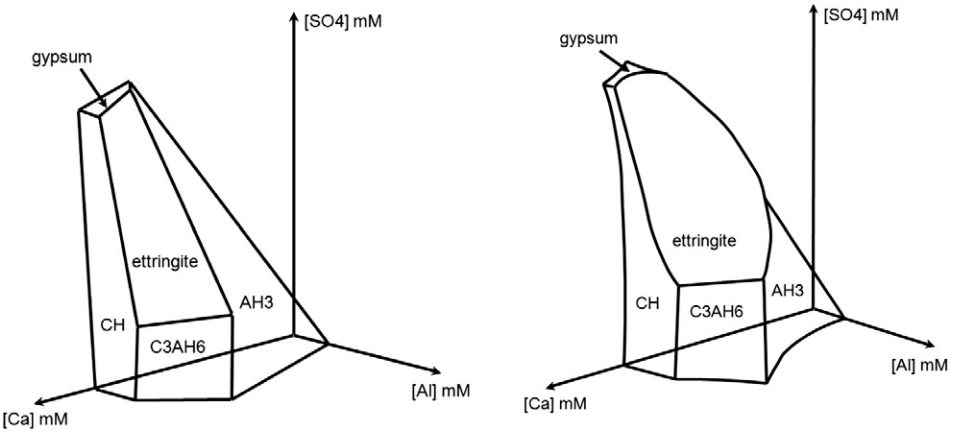

Fig. 3. Calculated phase diagram of the $CaO–Al_2O_3–CaSO_4–H_2O$ system at T = 25 °C and P = 1 bar (right) and the same phase diagram simplified by plotting with straight lines connecting the invariant points (left) [103].

effects of changes in the composition of the starting materials, or of temperature, or both can be assessed rapidly.

In recent years, the number of publications based on the application of thermodynamic methods in cement science has increased showing the increasing acceptance of thermodynamics as a tool to complement, or even replace, experiment. The use of thermodynamic calculations allows the influence of a large number of variables to be taken into account, *e.g.* the impact of changes in the composition of the starting materials [58,107–109] or of temperature [16,35] on the phase assemblage of cement systems. Combined with numerical values for the density of the relevant solids [35,36,110], thermodynamic modelling also allows calculation of the volume of the different phases and thus total porosity [58,108,111]. Porosity is a major parameter affecting mechanical strength of cement pastes as well as the permeability and diffusion of ions within the matrix [112–114]. Studies involving parameter variations have been carried out, *e.g.* on the influence blending of Portland cements with limestone [58,108], with additional sulphate [105,115], with slag [107,116,117], with fly ash [111,117,118] or with silica fume [117] and some of them are reported thereafter as examples.

One of the most striking findings arising from the application of thermodynamics to cement hydration has been the extent to which the hydrate phase equilibrium, with one conspicuous exception, achieves equilibrium. The exception is of course the persistence of an amorphous C–S–H which is metastable with respect to crystalline calcium silicate hydrates. However computational routines can accept a metastable phase and, given thermodynamic data for C–S–H, readily reproduce experimental results of the metastable equilibration of C–S–H with crystalline phases. In examples thus far studied experimentally the crystalline phases (CH, AFm, AFt …) readily equilibrate with each other as well as with C–S–H: in this context, "readily" implies days or weeks, possibly months where decreasing temperature drives reaction.

3.3.1. Influence of limestone

The addition of limestone fillers to clinker is increasingly common as it reduces the carbon footprint of cement systems. Limestone, rather than being inert, takes part in the hydration reaction. The addition of limestone to C_3A clinker or to Portland cements stabilises calcium monocarboaluminate hydrate, $C_4A\overline{C}H_{11}$ (monocarboaluminate), and ettringite, $C_6A\overline{S}_3H_{32}$, whilst monosulphate, $C_4A\overline{S}_3H_{12}$, is destabilised [58,119–121]:

$$C_3A + C\overline{C} + 11\,H \iff C_4A\overline{C}H_{11} \quad (10)$$

$$3C_4A\overline{S}H_{12} + 2\,C\overline{C} + 18\,H \iff C_6A\overline{S}_3H_{32} + 2C_4A\overline{C}H_{11} \quad (11)$$

$$\left(3*309 + 2*37 \iff 707 + 2*262\mathrm{cm}^3/\mathrm{mol}\right)$$

$$\left(1001 \iff 1231\mathrm{cm}^3/\mathrm{mol}\right).$$

In addition, ettringite can incorporate up to 9% of carbonate at 25 °C [16], which would further enhance the space-filling properties of the solids.

Thermodynamic modelling [58,108,111] supports these observations and illustrates that the presence of limestone stabilises ettringite; the presence of small amounts of limestone (up to approx. 5%) increases the total volume of hydrated solids and thus lowers the total porosity, as shown in Fig. 4A. But calcite in excess of that required to saturate the solids dilutes the other hydrates and the total volume of the hydrates decreases. The presence of more Al_2O_3 (and possibly Fe_2O_3) increases the scope for calcite reaction by (i) destabilising monosulphate in favour of monocarboaluminate, and (ii) combining displaced sulphate, together with a certain amount of carbonate (not shown in the above formulae), as ettringite. The total amount of

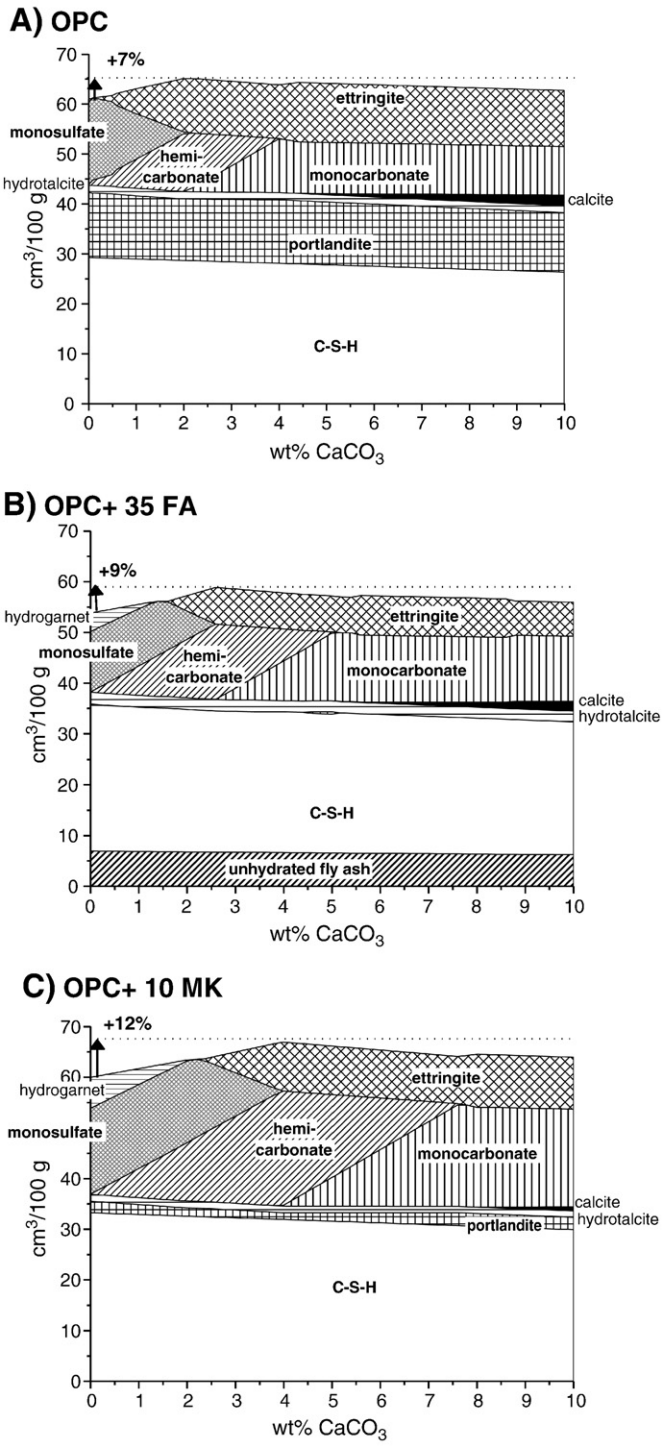

Fig. 4. Calculated volume changes as a function of the amount of limestone in hydrated A) Portland cement, B) PC + 35% fly ash (50% reacted); fly ash: CaO 6.3, SiO_2 50, Al_2O_3 24 wt.% [111], C) 90 PC — 10% metakaolin.

(reacted) Al_2O_3 increases from 5.3 wt.% in Portland cement (Fig. 4A) to 6.7 wt.% in the PC-fly ash (4B) and to 9.4 wt.% in a PC-metakaolin blend (4 C), although the amount of SO_3 remains nearly constant, ~3.8 wt.%. More Al_2O_3 should therefore result in more ettringite in the presence of limestone, increasing the total volume and decreasing the volume of the residual porosity compared to the PC used as the basis for calculation of Fig. 4A.

Experimental observations in Portland cements confirm the calculated reduction in porosity and concomitant increase in compressive strength in the presence of small amounts of limestone

([58,111,122–124] and Fig. 5A). The significance of the effect of limestone additions on Portland cements depends on cement composition and hydration time. At higher quantities of added limestone, limestone acts principally as a filler whilst the reduction of the amount of reactive clinker increases the porosity in the hydrated pastes and reduces the compressive strength (Fig. 5A). In a Portland cement blended with 35% fly ash (which contains 24 wt.% Al_2O_3 [111,124]) a similar increase in compressive strength was observed as in unmodified Portland cement mortar (5.4 wt.% Al_2O_3) (Fig. 5A). Detailed investigation indicated that only 35 to 40% of the fly ash had reacted [111,124], and thus a similar amount of Al_2O_3 was available for AFt formation (approx. 5.6 wt.%) as in the OPC paste.

Thus for each cement composition, an optimum limestone addition exists. This optimum is a complex function of cement sulphate and alumina contents. The same principle applies to blended cements but it is necessary also to take into account the slow release of alumina from substances such a fly ash. The combined addition of metakaolin (46 wt.% Al_2O_3) and limestone was observed to have a very pronounced positive effect on the compressive strength up to 28 days [126], in agreement with the thermodynamic calculations shown in Fig. 4C.

As discussed above, the influence of limestone is amplified by high Al_2O_3 (and possibly Fe_2O_3) contents. But the amount of SO_3 defined in terms of the SO_3/Al_2O_3 ratio also plays an important role. A high SO_3/Al_2O_3 ratio results in relatively more ettringite and less monosulphate, so the influence of limestone is less pronounced, as shown in Fig. 6 for calcium sulphoaluminate (C$A) cements. Calcium sulphoaluminate cements contain ye'elimite ($C_4A_3\bar{S}$) as a major constituent which reacts together with calcium sulphate to form ettringite, monosulphate and $Al(OH)_3$, depending on the $CaSO_4$ to $C_4A_3\bar{S}$ ratio. Depending on the clinker composition, additional hydration products such as strätlingite (C_2ASH_8), C–S–H or CAH_{10} precipitates [127–134]. Thermodynamic modelling of C$A systems has been applied [109,127–133]. In agreement with experimental data, thermodynamic modelling of C$A systems predicts mainly the formation of monosulphate and $Al(OH)_3$ if less than ~10 wt.% of $CaSO_4$ is used; in the presence of more of $CaSO_4$ more ettringite is formed (*cf.* Fig. 6, [109,129–131]). The presence of belite [128,131] or OPC [129] is calculated to reduce the amount of AH_3 whilst C–S–H and strätlingite [128,129] or C–S–H and siliceous hydrogarnet [131] are calculated to form. Blending with limestone leads, as discussed above, to the formation of monocarbonate and ettringite from monosulphate and calcite ([129,133], Fig. 6). In practice, the addition of limestone has been observed to increase the 28 day compressive strength of mortar samples by 10–15% at 20 °C and by 25–35% at 5 °C [133].

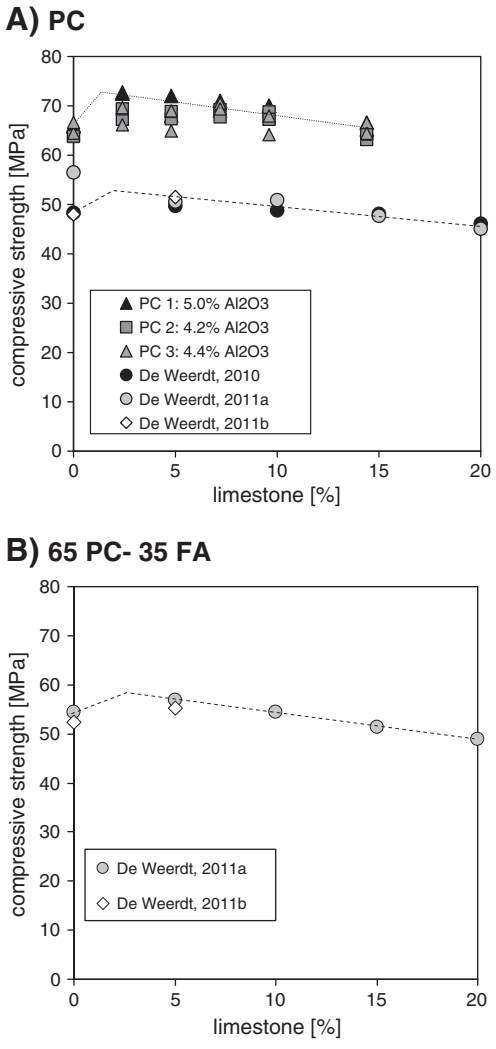

Fig. 5. Influence of the addition of small amounts of limestone on the compressive strength of A) hydrated Portland cement mortar after 28 days (PC 1, PC 2, PC3 (cement composition in [125]) and De Weerdt [123]) and 90 days (De Weerdt [124], [114]) and B) hydrated 65 Portland cement — 35% fly ash mortars. The lines are intended as eye guides only.

3.3.2. PC blended with SiO_2 rich materials

The main processes taking place during the hydration of Portland cements (PC) are well known (see Taylor [134]). The anhydrous

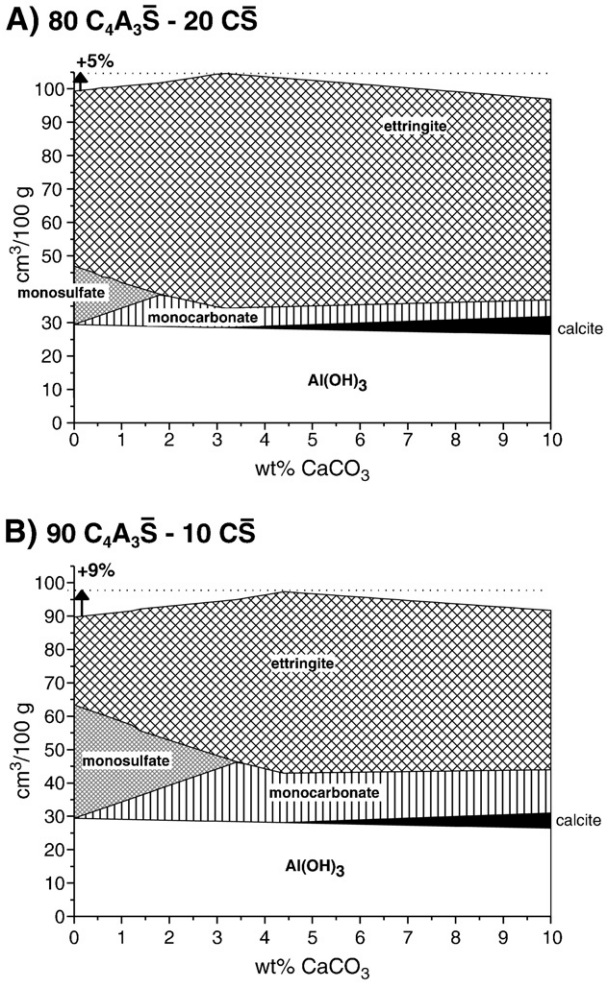

Fig. 6. Calculated volume changes as a function of the amount of limestone ($CaCO_3$) in a fully hydrated calcium sulfoaluminate (C$A) cement. A) 80 wt.% ye'elimite ($C_4A_3\$$), 20% anhydrite (C$), B) 90 wt.% ye'elimite ($C_4A_3\$$), 10% anhydrite (C$)).

clinker phases hydrate at various rates and the main hydrates formed are C–S–H, portlandite, ettringite and AFm phases. The blending of SCMs with Portland cement leads to a more complicated system where the hydration of the Portland cement and the reaction of the SCM occur simultaneously and influence the reactivity of each other. The reaction of most SCMs is slower than the reaction of the clinker phases and is influenced strongly by the pH of the aqueous phase [135–137] and by temperature [138–141]. The use of silica-rich SCMs influences the amount and kind of hydrates formed and thus the volume, porosity, strength and ultimately the durability. At the levels of substitution normally used, major changes are (i) a decrease in portlandite content and (ii) a lowering of the Ca/Si ratio in the C–S–H phase [140–145]. Alumina-rich SCMs increase the Al-uptake in C–S–H and the amount of aluminate hydrates. In general, the changes in the phase assemblages observed experimentally are well captured by thermodynamic modelling (*e.g.* [107,111,116–118] and Fig. 7) as detailed in a recent review on PC blended with supplementary cementitious materials [117].

3.4. Practical applications of thermodynamics applied to cement hydration

The composition and performance of Portland cements placed on the market are driven by a number of factors. These include the design and performance of the plant, the raw materials and fuel for clinker production, and the availability of SCMs for cement production. The cement producer must balance the need to minimise unit costs and maximise output at product quality requirements set by the market, and as specified in the relevant cement and application standards.

Nowadays most clinkers are produced in a fairly standardised plant (vertical raw mill, precalciner kiln, ball or even vertical cement mill with high efficiency separator). This produces a fairly standardised clinker with about 60% C_3S, 20% C_2S, 8% C_3A, and 10% C_4AF, as calculated by the Bogue equation [146], and a fairly standardised Portland cement with a fineness in the region 400 m^2/kg and low 45 μm residue. The C_3S content in the clinker ensures a sufficient content of alite for early strength. The relatively narrow size distribution of the cement resulting from the power-efficient grinding process contributes to acceptable 28 day strengths, but at the cost of a moderately high water demand. Probably the main differences that are found between modern clinkers today result from differences in the alkali content in the raw materials, and the sulphur content in the fuel. This variability results in wide ranging SO_3/alkali ratios, commonly referred to as the sulphatisation degree. Low SO_3/alkali ratios result in low contents of water soluble alkalis where much of the K_2O is incorporated into the belite phase and Na_2O is incorporated into the C_3A phase. At high SO_3/alkali ratios most of the alkalis are present in a soluble form, mainly as aphthitalite and calcium–langbeinite, although the concentration of SO_3 in belite also increases. This can lead to higher belite reactivity but, because the SO_3 thermodynamically stabilises belite, mineralisers are often needed to enhance alite formation.

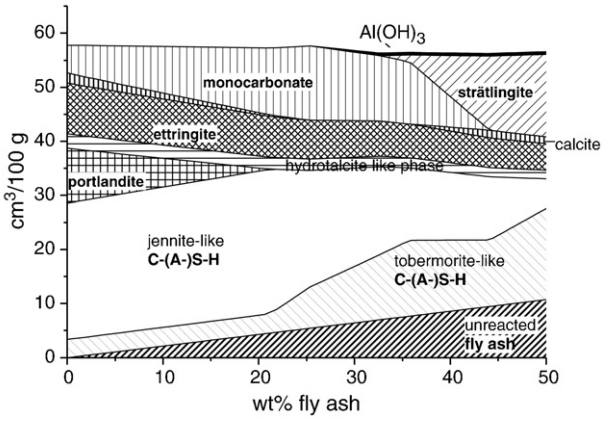

Fig. 7. Modelled changes in hydrated blended Portland cement with fly ash, assuming complete reaction of the Portland cement and 50% reaction of a low Ca fly ash (CaO 4.4, SiO_2 54, Al_2O_3 31 wt.%).
From [117].

3.4.1. The sulpho-aluminate reactions

The performance of a Portland cement in terms of setting behaviour and hydration is highly dependent on the above factors. As a consequence a better understanding of the hydration reactions and the underlying thermodynamics is important to achieve the correct addition of sulphate to the cement mill. The aqueous phase composition at the very beginning of cement hydration depends on the rates of dissolution of clinker and calcium sulphate phases. Thus depending on these rates of dissolution, the aqueous phase composition can be more or less supersaturated with respect to the hydrates that are likely to precipitate. If, for example, the C_3A is highly reactive (*e.g.* as occurs in low sulphate clinker with a high concentration of Na incorporated in the C_3A), sufficient readily soluble sulphate is needed to reach high enough sulphate concentrations in order to form early ettringite rather than the hydroxyl-AFm or monosulphate-AFm, *i.e.* where hydration takes place at invariant point "a" rather than "b" in Fig. 8. This diagram is constructed in the same way as Fig. 3 but using the thermodynamic data for SO_3-AFm and OH-AFm rather than hydrogarnet (C_3AH_6) [103]. This is a more accurate representation of the aluminate reactions in Portland cement where hydrogarnet is not observed to form as an early hydration product, as discussed previously. The concentration of calcium sulphate will remain constant at the invariant point (for our purposes we can assume that the alkali concentration is constant so we can treat the conditions as essentially invariant) until the gypsum is consumed, generally within a few hours. At this stage the concentration of sulphate falls, and the aqueous phase composition moving along the univariant curve connecting the invariant points "a" and "b" as ettringite continues to form. When the sulphate concentration decreases to invariant point "b", the composition of the pore solution is once again fixed and the SO_3-AFm phase forms whilst ettringite is consumed. This reaction continues for several days or even months until all of the available alumina from the clinker phases (and SCM such as fly ash) are exhausted. The point at which ettringite formation ceases (invariant point "b") is usually reached between 12 and 24 h. The optimum sulphate content for 1 day strength usually corresponds to this point being reached at closer to 12 than 24 h and may be related to local expansion in the hardening paste [147]. Higher aluminate contents in the Portland cement generally require more attention to sulphate optimisation because more ettringite can potentially form. At C_3A contents higher than 10%, optimum SO_3 contents for maximum strength often exceed the limits set by cement standards (e.g. 3.5% in ASTM C150, and 4.0% in EN-196-1).

3.4.2. The carbo-aluminate reactions

As described previously, carbonates will replace the sulphate in the AFm phase, but this reaction may take place after several days or weeks, and therefore cannot be used to optimise setting and early strengths. However, it can be used to optimise late strengths, as shown in Figs. 4A and 5A. The optimum strength appears to correspond to about 2 to 3% limestone at normal C_3A contents. From this, it would be reasonable to assume that optimum late strengths can be achieved at higher limestone contents if the aluminate content could be increased. Unfortunately, higher clinker C_3A contents in the clinker cannot be targeted for this because this would require excessive sulphate contents for optimum early hydration, as described in the previous section. The additional alumina should therefore only become available during medium to long term hydration. One method of achieving this is to increase the amount

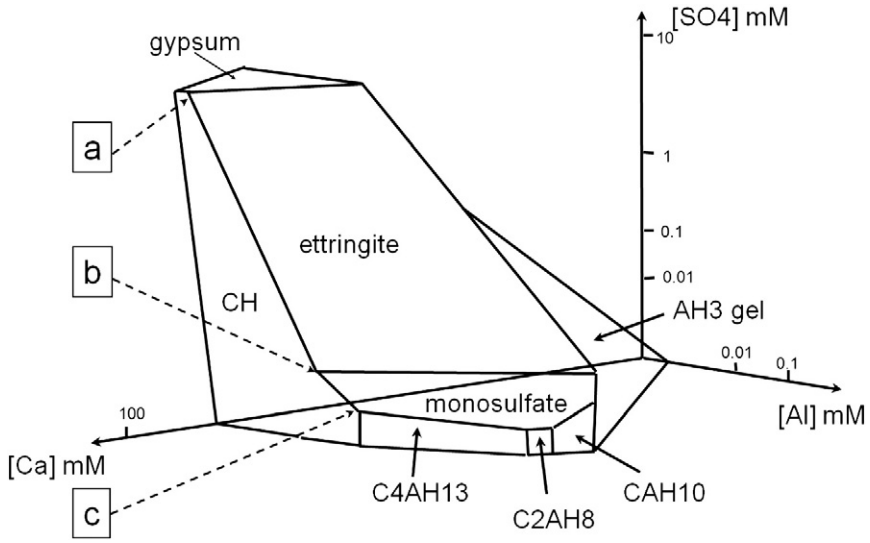

Fig. 8. Phase diagram of the $CaO–Al_2O_3–CaSO_4–H_2O$ system at T 25 °C modified from Fig. 3 showing the possibly metastable AFm phases that form instead of hydrogarnet.

of available alumina from the ferrite phase for example by increasing the solubility of iron with a complexing agent such as TIPA (tri isopropanol amine) which is finding increasing use as a grinding aid for cement milling [148]. Not surprisingly, this type of grinding aid seems to be most effective in limestone cements. Other sources of alumina for medium to long term hydration include the aluminosilicate SCMs and blast furnace slag; the higher the amount of available alumina, the higher the content of limestone for optimum strength as shown in Fig. 4B and C. This fact has not been lost to the industry: one of the most common types of cement in Europe is CEM II M, which in most cases contains mixtures of limestone and fly ash or limestone and slag. In many parts of the world, including Europe, where good quality fly ash and slag are already fully utilised this synergetic effect can effectively lower the clinker content in blended cements for the same performance, at least in terms of 28 day strengths, which remains the most important property (for good or bad) used to rank the competitive value of a cement. One of the most effective aluminosilicates for this reaction is metakaolin, not just because it is highly reactive in its own right, but because being a 1:1 clay it contains twice as much alumina as the more common 2:1 clays. Calcined 2:1 clays (SiO_2/Al_2O_3) normally have similar performance to fly ash which itself originates from 2:1 clays typically present in hard coals. The effect on strengths is illustrated in Fig. 9A and B. Although the calculations show that significantly less than 10% limestone reacts, optimum limestone contents for optimum strengths are in the region of 15% in the 1:1 clay (metakaolin) blend and 10% in the 2:1 clay (calcined smectite) blend (Fig. 10).

3.4.3. The pozzolanic reaction

Fly ash is clearly the most abundant pozzolan used today, but is a limited resource in most parts of the world, with the US and China as notable exceptions. Natural pozzolans, including calcined clays, can be increasingly used to address this, but the fact remains, as discussed below, that the pozzolanic reaction is limited to clinker replacement levels of about 25%. Whilst thermodynamics does not necessarily provide a solution to this it does go a long way to explaining the underlying cause. The relationship between the hydrate phase assemblages and the content of a typical siliceous fly ash of up to 50% (Fig. 11) offers some insight into the performance of Portland fly ash cements. Unpublished results showed Danish fly ashes to have 28 day activity indexes (defined in the European standard for fly ash, EN 450–1) in the region of 85 to 90% with the best practice relationship shown in Fig. 11 for EN 196 strengths as fly ash replaces up to 40% Portland cement in laboratory-prepared Portland fly ash cements. Some of the highest activities were reported for Australian fly ashes by Douglas and Pouskouleli [149] giving the relationship shown in Fig. 11. The relationship for the Danish ashes agrees with the 28 day concrete results reported by Ravina and Mehta [150]. The relationship for ashes with zero activity is also shown (inert filler, reported in [151]). At first glance these results are not in good agreement with the theoretical volumes of the hydrate assemblages

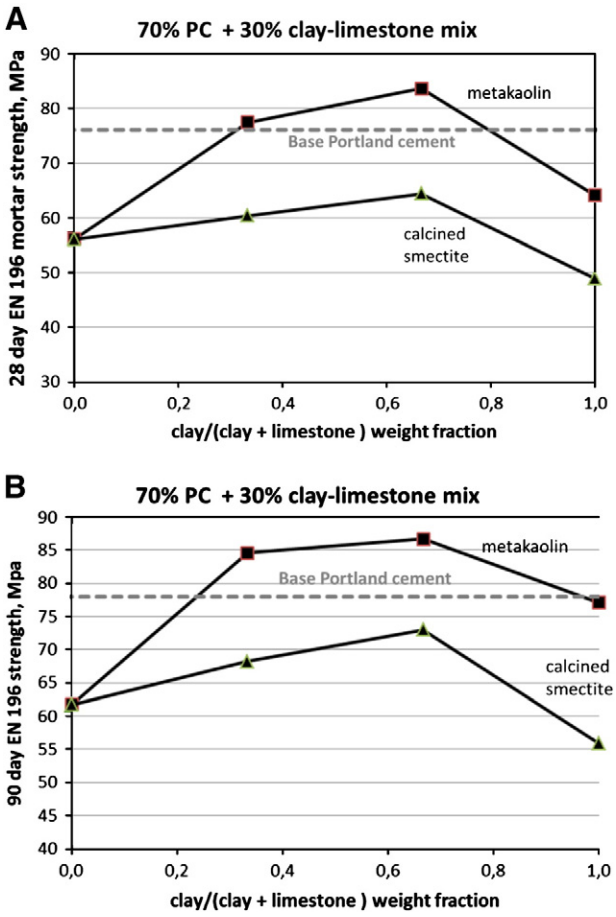

Fig. 9. EN 196 mortar strengths for Portland blended cement predicted from the thermodynamic model showing the synergetic effect of limestone and calcined clay. Fig. 9A and B shows the 28 day and 90 day mortar strengths respectively.

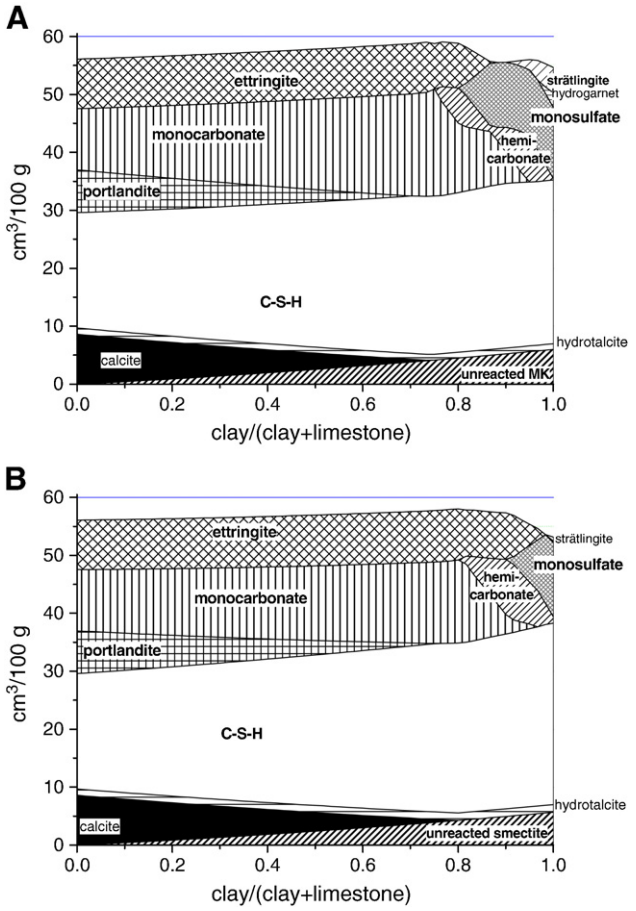

Fig. 10. Calculated volume changes as a function of limestone and calcined clay A) Portland cement +30% (metakaolin + limestone), B) Portland cement +30% (calcined smectite + limestone). 50% of clay reacted.

shown in Fig. 7, which assume 50% reaction of the fly ash, *i.e.* not an unrealistic degree of reaction at 28 days for a good quality siliceous fly ash. The theoretical volumes would indicate more or less constant porosity and strength at least up to 50% replacement, but the trends shown in Fig. 11 indicate that the fly ash has little more than a filler effect at replacement levels above about 25%. This more or less corresponds with the predicted formation of strätlingite indicating either that strätlingite does not make a significant contribution to strength or that its formation is kinetically sluggish. An alternative explanation is that the fly ash becomes less reactive as the pH of the pore solution drops as the concentration of calcium hydroxide and alkalis decline. Whatever the explanation, it is clear that the

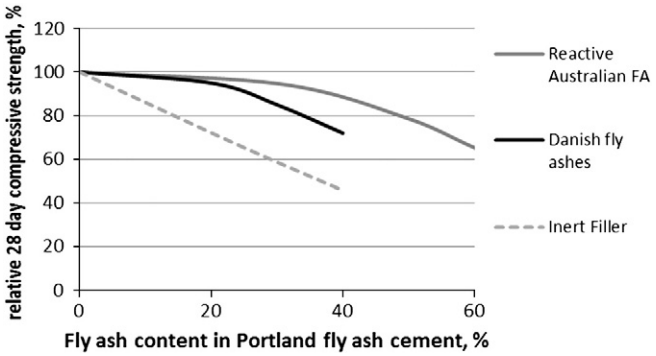

Fig. 11. Relationship between mortar strengths and fly ash contents at constant ratio of water to cementitious material, and constant content by weight of cementitious material.

thermodynamic predictions are insufficient on their own, and kinetic factors are largely responsible for the lack of performance of fly ash at replacement levels higher than 25%. Of course, fly ashes are known to provide better performance at later ages than 28 days with 50% fly ash providing equal strengths (*i.e.* corresponding to an activity index of 100%) at ages of 6 to 12 months, as reported for example in [150], but this is of little value to the cement or concrete producer when 28 day concrete strengths are commonly specified (and where the concrete needs to be brought into service at this age). The cement industry is therefore faced with the challenge of maximising the use of fly ash which in many parts of the world is a limited resource. In Europe for example the production of Portland cement clinker outstrips the production of fly ash by a ratio of 10 to 1 [152], however a large volume of this fly ash is used in cement types that allow contents well over 25% (CEM II/B V,W and CEM IV cements in the European cement standard EN 197–1). This makes little sense where the performance of the fly ash in terms of the pozzolanic reactions and strength provides little value at contents higher than 25%. It would therefore make most sense to limit the contents of fly ash in cements to 25% (as the concrete standards already do in several European countries).

4. Conclusion

Thermodynamics applied to cement science and especially to cement hydration is very successful and valuable if used with caution. Thus it would be very important to benchmark thermodynamic databases associated to their geochemical codes in order to have an international validation of their relevance. Indeed thermodynamic calculations have shown the sensitivity of mineral assemblages to temperature. Even relatively small temperature changes, in the range 0–40 °C, lead to substantial redistribution of anions such as OH^-, SO_4^{2-} and CO_3^{2-} amongst phases. Examples include the stabilisation of OH^- in AFm phases at lower temperatures with C_4AH_{13} becoming stable at <8 °C, the great stability of carbonate substitution in AFt (ettringite) phase at lower temperatures and the absolute destabilisation of hydrogarnet, C_3AH_6, in the presence of sulphate. Never again will we be able to think of the mineral composition of hydrated Portland cement as constant in a non-isothermal service environment. Moreover we see from a comparison of calculation and experiment that "kinetics" is not necessarily an insuperable barrier to engineering the phase composition of a hydrated Portland cement. This knowledge gives a powerful incentive to the development of links between the mineralogy and engineering properties of hydrated cement paste. Moreover, despite more than a century of research on this field, this paper demonstrated that some major improvements are still to come, such as a better understanding and treatment of solid solutions and of taking into account the water-unsaturated state of most of the cement paste contained in concrete. It also should not be forgotten that thermodynamics can also supply important parameters used to assess the kinetics of reactions. On the other hand, it must be remembered that the final state defined by thermodynamics is, in reality, often dependent on the kinetics of the chemical reactions, which, in turn, are influenced by the availability of reactants.

Looking ahead it can be said that the closed system behaviour of cements, particularly their mineralogical evolution with time as more blending agents such as fly ash and slag react, will be the focus of attention. The mineralogical evolution will be related to the evolution of porosity and permeability, as well as strength. Of course some of these parameters are not an intrinsic part of thermodynamics but are nevertheless important to engineering applications. These and other studies of closed system performance will serve to benchmark studies of cement performance in open systems.

We also have to remember that cement paste is thermodynamically unstable in most if not all service environments. The ensuing reactions are driven by free energy differences but the detailed expression of changing equilibrium is often moderated by the porosity, permeability

and microstructure of the paste as well as the macrostructure of the paste-aggregate system. Thus it is necessary to couple transport with reaction, as was described in a previous ICCC paper [153].

At the very least, the introduction of non-thermodynamic parameters is clearly essential to describe the engineering properties such as compressive and flexural strength but, at the same time, melding different types of data creates problems in developing correlations between the different types of data. It should be noted that our *quantitative* understanding of how many features, events and processes affect the future performance of cement and concrete is limited. If modelling does nothing more than force a more quantitative understanding of these features, processes and events, it will signal a considerable advance. Indeed, the nuclear industry has made and is making considerable strides in this direction. Computer routines are being used to predict performance lifetimes for cement and concrete used in nuclear structures. The goals of the nuclear industry do not always coincide with those of more conventional construction but considerable technology transfer is possible. In more conventional construction, goals for the immediate future must include optimisation of cement performance, so that the cost and environmental impact of cement production and use are reduced, whilst at the same time, the performance lifetime of blended cements is enhanced, thus reducing environmental impacts.

Acknowledgements

This paper has been prepared in the framework of the 13th International Conference on the Chemistry of Cement, 3 to 8 July 2011 in Madrid. The authors would like to express their thanks the organiser to initiate this paper and extend their thanks to Klaartje de Weerdt, SINTEF, for its support and helpful discussions and Belay Dilnesa, Empa and to Thomas Schmidt, Holcim, for preparation and analysis of thaumasite samples.

References

[1] H. Le Chatelier, Experimental Researches on the Constitution of Hydraulic Mortars, Kessinger Publishing, ISBN–10: 1436898862, 1905, 144 pp.
[2] H.H. Steinour, The reactions and thermochemistry of cement hydration at ordinary temperature. 3rd ICCC, London, Cement and Concrete Association (1952) 261–289.
[3] G.E. Bessey, The Calcium Aluminate and Silicate Hydrates, 2nd ICCC, Stockholm, Sweden, 1938, pp. 178–215.
[4] T. Thorvaldson, F.W. Birss, K.G. McCurdy, Calcium exchange in systems of $xCaO \cdot SiO_2 \cdot yH_2O$–$Ca(OH)_2$–$H_2O$, Chemistry of Cement, 1, 4th ICCC, Washington, 1960, pp. 315–319.
[5] A. Klein, P.K. Mehta, Nature of hydration products in the system $4CaO \cdot 3Al_2O_3$–SO_3–$CaSO_4$–CaO–H_2O, 5th ICCC. Tokyo, 4, 1968, pp. 336–340.
[6] P.W. Brown, The implications of phase equilibria on hydration in the tricalcium silicate–water and the tricalcium aluminate–gypsum–water systems, 8th ICCC. Rio de Janeiro, 3, 1986, pp. 231–238.
[7] D. Damidot, F.P. Glasser, Thermodynamic investigation of the CaO–Al_2O_3–$CaSO_4$–$CaCl_2$–H_2O system at 25 °C and the influence of Na_2O, 10th ICCC. Gothenburg, Sweden, 1997, 4 iv066.
[8] H.M. Jennings, C.M. Neubauer, K.D. Breneman, B.J. Christensen, Phase diagrams relevant to hydration of C3S. Part 1: A case for metastable equilibrium, 10th ICCC. Gothenburg, Sweden, 1997, 2ii057.
[9] J.A. Gisby, R.H. Davies, A.T. Dinsdale, M. Tyrer, F.P. Glasser, J. Hill, P. Livesey, C. Walker, C–S–H solubility modelling at different temperatures, 12th ICCC. Montreal, Canada, 2007, W1-05.4.
[10] R.J.Kirkpatrick and X.-D. Cong, An Introduction to 27Al and 29Si NMR Spectroscopy of Cements and Concretes, in Application of NMR Spectroscopy to Cement Science, 55–75, Gordon and Breach Reading England
[11] J. Skibsted, Hydration Kinetics for the alite, belite and calcium aluminate phases in Porland cement from 27Al and 29Si MAS NMR spectroscopy, 10th ICCC, Gothenburg, Sweden, 1997, 2ii056.
[12] M. Hillert, in: Y.A. Chang, J.F. Smit (Eds.), Calculation of Phase Diagrams and Thermochemistry of Alloy Phases, Met. Soc AIME, 1979.
[13] L. Kaufman, H. Bernstein, Computer Calculation of Phase Diagrams, Academic Press, New York, 1970.
[14] V.I. Babushkin, G.M. Matveyev, O.P. Mchedlov-Petrossyan, Thermodynamics of Silicates, Springer-Verlag, Berlin, 1985, 459 pp.
[15] N. Saunders, A.P. Midownik, CALPHAD, A Comprehensive Guide, Elsevier, 1998.
[16] T.Matschei, Thermodynamics of Cement Hydration, PhD Thesis University of Aberdeen 221pp, 2009
[17] T. Matschei, F.P. Glasser, Temperature dependence, 0 to 40 °C, of the mineralogy of Portland cement paste in the presence of calcium carbonate, Cement and Concrete Research 40 (5) (2010) 763–777.
[18] B. Lothenbach, D. Damidot, T. Matschei, J. Marchand, Thermodynamic modelling: state of knowledge and challenges, Advances in Cement Research 22 (4) (2010) 211–223.
[19] H.C. Helgeson, J.M. Delany, H.W. Nesbitt, D.K. Bird, Summary and critique of the thermodynamic properties of rock-forming minerals, American Journal of Science 278-A (1978) 1–229.
[20] J.W. Johnson, E.H. Oelkers, H.C. Helgeson, SUPCRT92: a software package for calculating the standard molal thermodynamic properties of minerals, gases, aqueous species, and reactions from 1 to 5000 bar and 0 to 1000 °C, Computers & Geosciences 18 (7) (1992) 899–947.
[21] R.A. Robie, B.S. Hemingway, Thermodynamic properties of minerals and related substances at 298.15 K and 1 bar (10^5 Pascals) pressure and at higher temperatures: U. S, Geological Survey Bulletin 2131 (1995).
[22] E.L. Shock, D.C. Sassani, M. Willis, D.A. Sverjensky, Inorganic species in geologic fluids: correlations among standard molal thermodynamic properties of aqueous ions and hydroxide complexes, Geochimica et Cosmochimica Acta 61 (5) (1997) 907–950.
[23] D.A. Sverjensky, E.L. Shock, H.C. Helgeson, Prediction of the thermodynamic properties of aqueous metal complexes to 1000 °C and 5 kb, Geochimica et Cosmochimica Acta 61 (7) (1997) 1359–1412.
[24] W. Hummel, U. Berner, E. Curti, F.J. Pearson, T. Thoenen, Nagra/PSI chemical thermodynamic data base 01/01, USA, also published as Nagra Technical Report NTB 02–16, Universal Publishers/uPUBLISH.com, Wettingen, Switzerland, 2002.
[25] V.I. Babushkin, O.P. Matveev, O.P. Mčedlov-Petrosjan, Thermodinamika Silikatov, Strojisdat, Moskau, 1965.
[26] V.M. Nikushchenko, V.S. Khotimchenko, P.F. Rumyantsev, A.I. Kalinin, Determination of the standard free energies of formation of calcium hydroxyaluminates, Cement and Concrete Research 3 (1973) 625–632.
[27] P. Barret, D. Bertrandie, D. Beau, Calcium hydrocarboaluminate, carbonate, alumina gel and hydrated aluminates solubility diagram calculated in equilibrium with CO_{2g} and with Na^+_{aq} ions, Cement and Concrete Research 13 (1983) 789–800.
[28] E.J. Reardon, An ion interaction model for the determination of chemical equilibria in cement/water systems, Cement and Concrete Research 20 (1990) 175–192.
[29] E.J. Reardon, Problems and approaches to the prediction of the chemical composition in cement/water systems, Waste Management 12 (1992) 221–239.
[30] D.G. Bennett, D. Read, M. Atkins, F.P. Glasser, A thermodynamic model for blended cements. II: cement hydrate phases; thermodynamic values and modelling studies, Journal of Nuclear Materials 190 (1992) 315–325.
[31] F.B. Neall, Modelling of the Near-Field Chemistry of the SMA Repository at the Wellenberg Site. PSI, 1994, p. 94-18.
[32] D. Damidot, S. Stronach, A. Kindness, M. Atkins, F.P. Glasser, Thermodynamic investigation of the CaO–Al_2O_3–$CaCO_3$–H_2O closed system at 25 °C and the influence of Na_2O, Cement and Concrete Research 24 (3) (1994) 563–572.
[33] X. Bourbon, Chemical conceptual model for cement based materials–mineral phases and thermodynamic data, ANDRA Technical Report C.NT.ASCM.03.026.A, 2003.
[34] B. Lothenbach, F. Winnefeld, Thermodynamic modelling of the hydration of Portland cement, Cement and Concrete Research 36 (2) (2006) 209–226.
[35] B. Lothenbach, T. Matschei, G. Möschner, F.P. Glasser, Thermodynamic modelling of the effect of temperature on the hydration and porosity of Portland cement, Cement and Concrete Research 38 (1) (2008) 1–18.
[36] T. Matschei, B. Lothenbach, F.P. Glasser, Thermodynamic properties of Portland cement hydrates in the system CaO–Al_2O_3–SiO_2–$CaSO_4$–$CaCO_3$–H_2O, Cement and Concrete Research 37 (10) (2007) 1379–1410.
[37] G. Möschner, B. Lothenbach, J. Rose, A. Ulrich, R. Figi, R. Kretschmar, Solubility of Fe-ettringite ($Ca_6[Fe(OH)_6]_2(SO_4)_3 26H_2O$), Geochimica et Cosmochimica Acta 72 (1) (2008) 1–18.
[38] G. Möschner, B. Lothenbach, A. Ulrich, R. Figi, R. Kretschmar, Solid solution between Al-ettringite and Fe-ettringite ($Ca_6[Al_{1-x}Fe_x(OH)_6]_2(SO_4)_3 26H_2O$), Cement and Concrete Research 39 (2009) 482–489.
[39] T. Schmidt, B. Lothenbach, M. Romer, K.L. Scrivener, D. Rentsch, R. Figi, A thermodynamic and experimental study of the conditions of thaumasite formation, Cement and Concrete Research 38 (3) (2008) 337–349.
[40] P. Blanc, X. Bourbon, A. Lassin, E. Gaucher, Chemical model for cement-based materials: temperature dependence of thermodynamic functions for nanocrystalline and crystalline C–S–H phases, Cement and Concrete Research 40 (6) (2010) 851–866.
[41] P. Blanc, X. Bourbon, A. Lassin, E. Gaucher, Chemical model for cement-based materials: thermodynamic data assessment for phases other than CSH, Cement and Concrete Research 40 (9) (2010) 1360–1374.
[42] T. Thoenen, D. Kulik, Nagra/PSI chemical thermodynamic database 01/01 for the GEM-Selektor (V.2-PSI) geochemical modeling code. PSI TM-44-02-09, 2003.
[43] M. Balonis, B. Lothenbach, G. Le Saout, F.P. Glasser, Impact of chloride on the mineralogy of hydrated Portland cement systems, Cement and Concrete Research 40 (7) (2010) 1009–1022.
[44] S.M. Leisinger, B. Lothenbach, G. Le Saout and C.A. Johnson, Solid solutions between monosulfate and monochromate $4CaO \cdot Al_2O_3 \cdot Ca[(CrO_4)_x(SO_4)_{1-x}] \cdot nH_2O$. Cement and Concrete Research, submitted for publication.
[45] S.M. Leisinger, B. Lothenbach, G. Le Saout, R. Kägi, B. Wehrli, C.A. Johnson, Solid solutions between CrO_4- and SO_4-ettringite $Ca_6(Al(OH)_6)_2(Cr_xS_{1-x}O_4)_3 * 26 H_2O$, Environmental Science & Technology 44 (23) (2010) 8983–8988.

[46] K. Rozov, U. Berner, C. Taviot-Gueho, F. Leroux, G. Renaudin, D. Kulik, L.W. Diamond, Synthesis and characterization of the LDH hydrotalcite–pyroaurite solid–solution series, Cement and Concrete Research 40 (8) (2010) 1248–1254.
[47] B.Z. Dilnesa, B. Lothenbach, G. Le Saout, G. Renaudin, A. Mesbah, Y. Filinchuk, A. Wichser, E. Wieland, Iron in carbonate containing AFm phases, Cement and Concrete Research 41 (2011) 311–323.
[48] D.A. Kulik, Improving the structural consistency of C-S-H solid solution thermodynamic models, Cement and Concrete Research 41 (2011) 477–495.
[49] K. Rozov, Personal communication, 2011.
[50] L. Aimoz, E. Wieland, B. Lothenbach, M.A. Glaus, E. Curti, Characterization and Solubility Determination of the Solid–Solution between AFm-I_2 and AFm-SO_4, NUWCEM, Avignon, France, 2011, 2011.
[51] B.Z. Dilnesa, B. Lothenbach, G. Le Saout, E. Wieland, K.L. Scrivener, Fe-containing hydrates in cementitious systems, ICCC 2011. Madrid, 2011.
[52] P. Blanc, P. Piatone, A. Lassin, A. Burnol, Thermochimie: Sélection de constantes thermodynamiques pour les éléments majeurs, le plomb et le cadmium, Rapport final: BRGM RP-54902-FR, 2006.
[53] P. Piatone, C. Nowak, P. Blanc, A. Lassin, A. Burnol, Themoddem: THERmodynamique et MOdélisation de la Dégradation DEchets Minéraux, Rapport d'avancement. BRGM/RP-54547-FR, 2006.
[54] D. Damidot, F.P. Glasser, Thermodynamic investigation of the CaO–Al_2O_3–$CaSO_4$–H_2O system at 25 °C and the influence of Na_2O, Cement and Concrete Research 23 (1993) 221–238.
[55] J.H. Lee, D.M. Roy, B. Mann, D. Stahl, Integrated approach to modeling long-term durability of concrete engineered barriers in LLRW disposal facility, Material Research Society Symposium Proceedings 353 (1995) 881–889.
[56] D. Rothstein, J.J. Thomas, B.J. Christensen, H.M. Jennings, Solubility behavior of Ca-, S-, Al-, and Si-bearing solid phases in Portland cement pore solutions as a function of hydration time, Cement and Concrete Research 32 (10) (2002) 1663–1671.
[57] C.J. Warren, E.J. Reardon, The solubility of ettringite at 25 °C, Cement and Concrete Research 24 (8) (1994) 1515–1524.
[58] B. Lothenbach, G. Le Saout, E. Gallucci, K. Scrivener, Influence of limestone on the hydration of Portland cements, Cement and Concrete Research 38 (6) (2008) 848–860.
[59] M. Paul, F.P. Glasser, Impact of prolonged warm (85 degrees C) moist cure on Portland cement paste, Cement and Concrete Research 30 (12) (2000) 1869–1877.
[60] T.H. Lilley and C.C. Briggs, Activity Coefficients of Calcium Sulphate in Water at 25 Â° C. Proceedings of the Royal Society of London. Series A, Mathematical and Physical Sciences, 349(1658) (1976) 355–368.
[61] G.M. Anderson, D.A. Crerar, Thermodynamics in Geochemistry: The Equilibrium Model, Oxford University Press, Oxford, 1993.
[62] D.K. Nordstrom, J.L. Munoz, Geochemical Thermodynamics, Blackwell, Boston, 1988.
[63] J. Ederova, V. Satava, Heat capacities of C_3AH_6, C_4ASH_{12} and $C_6AS_3H_{32}$, Thermochimica Acta 31 (1979) 126–128.
[64] D. Damidot, F.P. Glasser, Thermodynamic investigation of the CaO–Al_2O_3–$CaSO_4$–H_2O system at 50 °C and 85 °C, Cement and Concrete Research 22 (1992) 1179–1192.
[65] D.E. Macphee, S.J. Barnett, Solution properties of solids in the ettringite–thaumasite solid solution series, Cement and Concrete Research 34 (2004) 1591–1598.
[66] R.B. Perkins, C.D. Palmer, Solubility of ettringite ($Ca_6[Al(OH)_6]_2(SO_4)_3\cdot 26H_2O$) at 5–75 °C, Geochimica et Cosmochimica Acta 63 (13/14) (1999) 1969–1980.
[67] V. Satava, Determination of standard enthalpies and Gibbs' energies of formation for $6CaO.Al_2O_3.3SO_3.32H_2O$($C_6A\$H_{32}$) and $4CaO.Al_2O_3.12H_2O$($C_4A\$H_{12}$) by the DHA method, Silikaty 30 (1986) 1–8.
[68] H.A. Berman, E.S. Newman, Heat of formation of calcium aluminate monosulfate, Journal of Research of the National Bureau of Standards-A. Physics and Chemistry 67A (1) (1963) 1–13.
[69] D. Kulik, GEMS-PSI 2.1, PSI-Villigen, Switzerland, 2005. http://les.web.psi.ch/Software/GEMS-PSI/ available at.
[70] D. Kulik, Minimising uncertainty induced by temperature extrapolations of thermodynamic data: a pragmatic view on the integration of thermodynamic databases into geochemical computer codes, The use of thermodynamic databases in performance assessment, OECD, Barcelona, 2002, pp. 125–137.
[71] Y. Gu, C.H. Gammons, M.S. Bloom, A one-term extrapolation method for estimating equilibrium constants of aqueous reactions at elevated temperatures, Geochimica et Cosmochimica Acta 58 (17) (1994) 3545–3560.
[72] T. Schmidt, B. Lothenbach, M. Romer, K. Scrivener, Investigations of external sulfate attack on limestone blended Portland cements, Concrete in Aggressive Aqueous Environments — Performance, Testing and Modeling, Toulouse, France, 2009, pp. 37–44.
[73] F. Bellmann, On the formation of thaumasite $CaSiO_3.CaSO_4.CaCO_3.15H_2O$: Part I, Advances in Cement Research 16 (2) (2004) 55–60.
[74] J.S. Seewald, W.E. Seyfried, Experimental determination of portlandite solubility in H2O and acetate solutions at 100–350 °C and 500 bar: constraints on calcium hydroxide and calcium acetate complex stability, Geochimica et Cosmochimica Acta 55 (1990) 659–669.
[75] N. Meller, C. Hall, J.S. Phipps, A new phase diagram for the CaO–Al_2O_3–SiO_2–H_2O hydroceramic system at 200 °C, Material Research Bulletin 40 (2005) 715–723.
[76] A. Lassin, M. Azaroual, L. Mercury, Geochemistry of unsaturated soil systems: aqueous speciation and solubility of minerals and gases in capillary solutions, Geochimica et Cosmochimica Acta 69 (22) (2005) 5187–5201.
[77] L. Mercury, Y. Tardy, Negative pressure of stretched liquid water, Geochemistry of soil capillaries. Geochimica et Cosmochimica Acta 65 (20) (2001) 3391–3408.
[78] M. Pettenati, L. Mercury, M. Azaroual, Capillary geochemistry in non-saturated zone of soils. Water content and geochemical signatures, Applied Geochemistry 23 (12) (2008) 3799–3818.
[79] L. Mercury, M. Azaroual, H. Zeyen, Y. Tardy, Thermodynamic properties of solutions in metastable systems under negative or positive pressures, Geochimica et Cosmochimica Acta 67 (10) (2003) 1769–1785.
[80] D. Damidot, S.J. Barnett, F.P. Glasser, D.E. Macphee, Investigation of the CaO–Al_2O_3–SiO_2–$CaSO_4$–$CaCO_3$–H_2O system at 25 °C by thermodynamic calculation, Advances in Cement Research 16 (2) (2004) 69–76.
[81] F. Bellmann, D. Damidot, B. Möser, J. Skibsted, Improved evidence for the existence of an intermediate phase during hydration of tricalcium silicate, Cement and Concrete Research 40 (2010) 875–884.
[82] D. Damidot, Calculation of critically supersaturated domains with respect to ettringite in the CaO–Al_2O_3–$CaSO_4$–H_2O system at 20 °C, 12th International Congress on the Chemistry of Cement. Montreal, Canada, 2007, W1-05.5.
[83] D. Damidot, P. Barret, Calculation of the maximum supersaturation curve of C_2AH_8 in the CaO–Al_2O_3–H_2O system at 20 ° C, 10th ICCC. Gothenburg, Sweden, 1997, 2 ii024.
[84] J.J. van Laar, Zeit Phys Chem 63 (1908) 216.
[85] S. Börjesson, A. Emrén, C. Ekberg, A thermodynamic model for the calcium silicate hydrate gel, modelled as a non-ideal binary solution, Cement and Concrete Research 27 (11) (1997) 1649–1657.
[86] M. Djuric, M. Komljenovic, L. Petrasinovic-Stojkanovic, B. Zivanovic, Thermodynamic analysis of the C–S–H system, Advances in Cement Research 6 (1) (1994) 19–26.
[87] E. Gartner, H.M. Jennings, Thermodynamic of calcium silicate hydrates and their solutions, Journal of the American Ceramic Society 70 (1987) 743–749.
[88] S.A. Greenberg, T.N. Chang, Investigation of the colloidal hydrated calcium silicates. II. Solubility relationships in the calcium oxide–silica–water system at 25°, The Journal of Physical Chemistry 69 (1) (1965) 182–188.
[89] F.E. Jones, The quaternary system CaO–Al_2O_3–$CaSO_4$–H_2O. Equilibria with crystalline $Al_2O_3 3H_2O$, alumina gel, and solid solutions, The Journal of Physical Chemistry 48 (6) (1944) 311–356.
[90] F.E. Jones, The quinary system CaO–Al_2O_3–$CaSO_4$–K_2O–H_2O (1 per cent KOH), The Journal of Physical Chemistry 48 (6) (1944) 356–378.
[91] F.E. Jones, The quinary system CaO–Al_2O_3–$CaSO_4$–Na_2O–H_2O (1 per cent NaOH), The Journal of Physical Chemistry 48 (6) (1944) 379–394.
[92] O.P. Mchedlov-Petrossyan, V.L. Chernyavski, Thermodynamics of hydrate formation late stages in cement materials, Il Cemento 1 (1994) 25–32.
[93] M. Soustelle, B. Guilhot, A.A. Fournier, M. Murat, A. Negro, Application des proprietes thermodynamiques du systeme CaO–Al_2O_3–CO_2–H_2O a l'hydratation des ciments alumineux, Cement and Concrete Research 15 (4) (1985) 655–661.
[94] H.N. Stein, Thermodynamic considerations on the hydration mechanisms of Ca_3SiO_5 and $Ca_3Al_2O_6$, Cement and Concrete Research 2 (2) (1972) 167–177.
[95] L.S. Wells, E.T. Carlson, Hydratation of aluminous cements and its relation to the phase equilibria in the system lime–alumina–water, Journal of Research of the National Bureau of Standards 57 (6) (1956) 335–353.
[96] P.W. Brown, The system Na_2O–CaO–SiO_2–H_2O, Journal of the American Ceramic Society 73 (11) (1990) 3457–3461.
[97] J. D'Ans, H. Eick, Das System CaO–Al_2O_3–H_2O bei 20 °C und das Erhärten der Tonerdezemente, Zement-Kalk-Gips 6 (1953) 197–210.
[98] J. D'Ans, H. Eick, Das System CaO–Al_2O_3–H_2O bei 20 °C, Zement-Kalk-Gips 6 (1953) 302–311.
[99] E.P. Flint, L.S. Wells, Study of the system CaO–SiO_2–H_2O at 30 C and of the reaction of water on the anhydrous calcium silicates, Journal of Research of the National Bureau of Standards 12 (1934) 751–783.
[100] G.L. Kalousek, Studies of portions of the quarternary system soda–lime–silica–water at 25 °C, Journal of Research of the National Bureau of Standards 32 (1944) 285–302.
[101] H.H. Steinour, Aqueous cementitious systems containing lime and alumina, Research and Develop. Labs. Portland Cement. Assoc. Bull. 34 (1951) 1–97.
[102] L.S. Wells, W.F. Clarke, H.F. McMurdie, Study of the system CaO–Al_2O_3–H_2O at temperatures of 21° and 90 °C, Journal of Research of the National Bureau of Standards 30 (1943) 367–409.
[103] D. Damidot, Description d'une méthode pour calculer les diagrammes de phases solides-liquide. Application à l'étude de parties du système CaO–Al_2O_3–SiO_2–$CaSO_4$–$CaCO_3$–$CaCl_2$–Na_2O–K_2O–H_2O en relation avec l'hydratation du ciment, Habilitation Thesis, University of Burgundy, 185 pp. (1995).
[104] B. Albert, B. Guy, D. Damidot, Water chemical potential: a key parameter to determine the thermodynamic stability of some cement phases in concrete? Cement and Concrete Research 36 (5) (2006) 783–790.
[105] I. Juel, D. Herfort, R. Gollop, J. Konnerup-Madsen, H.J. Jakobsen, J. Skibsted, A thermodynamic model for predicting the stability of thaumasite, Cement & Concrete Composites 25 (2003) 867–872.
[106] E.P. Nielsen, D. Herfort, M.R. Geiker, Phase equilibria of hydrated Portland cement, Cement and Concrete Research 35 (2005) 109–115.
[107] M. Atkins, D.G. Bennett, A.C. Dawes, F.P. Glasser, A. Kindness, D. Read, A thermodynamic model for blended cements, Cement and Concrete Research 22 (2–3) (1992) 497–502.
[108] T. Matschei, B. Lothenbach, F.P. Glasser, The role of calcium carbonate in cement hydration, Cement and Concrete Research 37 (4) (2007) 551–558.
[109] F.P. Glasser, L. Zhang, High-performance cement matrices based on calcium sulfoaluminate–belite compositions, Cement and Concrete Research 31 (12) (2001) 1881–1886.
[110] M. Balonis, F.P. Glasser, The density of cement phases, Cement and Concrete Research 39 (9) (2009) 733–739.

[111] K. De Weerdt, M. Ben Haha, G. Le Saout, K.O. Kjellsen, H. Justness, B. Lothenbach, Hydration mechanisms of ternary Portland cements containing limestone powder and fly ash, Cement and Concrete Research 41 (3) (2011) 279–291.
[112] J.M. Galindez, J. Molinero, On the relevance of electrochemical diffusion for the modelling of degradation of cementitious materials, Cement and Concrete Research 41 (2011) 279–291.
[113] B. Lothenbach, B. Bary, P. Le Bescop, T. Schmidt, N. Leterrier, Sulfate ingress in Portland cements, Cement and Concrete Research 40 (8) (2010) 1211–1225.
[114] E. Samson, J. Marchand, J.J. Beaudoin, Modeling the influence of chemical reactions on the mechanisms of ionic transport in porous materials. An overview, Cement and Concrete Research 30 (12) (2000) 1895–1902.
[115] B. Lothenbach, T. Schmidt, Influence of limestone on sulfate ingression, Concrete in Aggressive Aqueous Environments. Performance, Testing and Modelling, Proceedings PRO 63, 1, RILEM Publications, Toulouse, France, 2009, pp. 212–219.
[116] M. Atkins, F.P. Glasser, A. Kindness, Phase relation and solubility modelling in the $CaO–SiO_2–Al_2O_3–MgO–SO_3–H_2O$ system: for application to blended cements, Material Research Society Symposium Proceedings 212 (1991) 387–394.
[117] B. Lothenbach, K. Scrivener, R.D. Hooton, Supplementary cementitious materials, Cement and Concrete Research, 2011, doi:10.1016/j.cemconres.2010.12.001.
[118] B. Lothenbach, E. Wieland, R. Figi, D. Rentsch and B. Schwyn, Hydration of blended cements. 17. Internationale Baustofftagung (ibausil). Weimar, Germany, 2009, Volume 1 1-0213-1-0218.
[119] H.-J. Kuzel, H. Pöllmann, Hydration of C_3A in the presence of $Ca(OH)_2$, $CaSO_42H_2O$ and $CaCO_3$, Cement and Concrete Research 21 (1991) 885–895.
[120] H. Kuzel, H. Baier, Hydration of calcium aluminate cements in the presence of calcium carbonate, European Journal of Mineralogy 8 (1996) 129–141.
[121] V.L. Bonavetti, V.F. Rahhal, E.F. Irassar, Studies on the carboaluminate formation in limestone filler-blended cements, Cement and Concrete Research 31 (2001) 853–859.
[122] D. Herfort, Limestone Additions, Workshop on Limestone Additions in Cement and Concrete, Copenhagen, Denmark, 2006.
[123] K. De Weerdt, H. Justness, K.O. Kjellsen, E. Sellevold, Fly ash-limestone ternary composite cements: synergetic effect at 28 days, Nordic Concrete Research 42 (2) (2010) 51–70.
[124] K. De Weerdt, K.O. Kjellsen, E. Sellevold, H. Justness, Synergy between fly ash and limestone powder in ternary cements, Cement and Concrete Composites 33 (1) (2011) 30–38.
[125] D. Herfort, S. Rasmussen, E. Jons, B. Osbaeck, Mineralogy and performance of cement based on high sulfate clinker, Cement Concrete and Aggregates 21 (1) (1999) 64–72.
[126] M. Antoni, J. Rossen, K. Scrivener, R. Castillo, A. Alujas Diaz and F. Martirena, Investigation of cement substitution by combined addition of calcined clays and limestone. Cement and Concrete Research, submitted for publication
[127] L. Zhang, F.P. Glasser, Hydration of calcium sulfoaluminate cement at less than 24 hours, Advances in Cement Research 14 (4) (2002) 141–155.
[128] F. Winnefeld, B. Lothenbach, Hydration of calcium sulfoaluminate cements: experimental findings and thermodynamic modelling, Cement and Concrete Research 40 (8) (2010) 1239–1247.
[129] L. Pelletier, F. Winnefeld, B. Lothenbach, The ternary system Portland cement – calcium sulphoaluminate clinker – anhydrite: hydration mechanism and mortar properties, Cement and Concrete Composites 32 (2010) 497–507.
[130] F. Winnefeld, S. Barlag, Calorimetric and thermogravimetric study on the influence of calcium sulfate on the hydration of ye'elimite, Journal of Thermal Analysis and Calorimetry 101 (3) (2010) 949–957.
[131] S. Berger, C. Cau Dit Coumes, P. Le Bescop, D. Damidot, Influence of a thermal cycle at early age on the hydration of calcium sulphoaluminate cements with variable gypsum contents, Cement and Concrete Research 41 (2) (2011) 149–160.
[132] M.C.G. Juenger, F. Winnefeld, J.L. Provis and J.H. Ideker, Advances in alternative cementitious binders. Cement and Concrete Research, 41 in press doi:10.1016/j.cemconres.2010.11.012.
[133] L. Pelletier, F. Winnefeld, B. Lothenbach and C.J. Müller, Beneficial use of limestone filler with calcium sulphoaluminate cement. Construction and Building Materials, submitted for publication
[134] H.F.W. Taylor, Cement Chemistry, Thomas Telford Publishing, London, 1997.
[135] B.R. Bickmore, K.L. Nagy, A.K. Gray, A.R. Brinkerhoff, The effect of $Al(OH)_4^-$ on the dissolution rate of quartz, Geochimica et Cosmochimica Acta 70 (2006) 290–305.
[136] P.M. Dove, The dissolution kinetics of quartz in sodiumchloride solutions at 25° to 300 °C, American Journal of Science 294 (1994) 665–712.
[137] M. Ben Haha, K. De Weerdt, B. Lothenbach, Quantification of the degree of reaction of fly ash, Cement and Concrete Research 40 (11) (2010) 1620–1629.
[138] S. Hanehara, F. Tomosawa, M. Kobayakawa, K.R. Hwang, Effects of water/powder ratio, mixing ratio of fly ash, and curing temperature on pozzolanic reaction of fly ash in cement paste, Cement and Concrete Research 31 (1) (2001) 31-19.
[139] L.Y. Gómez-Zamorano, J.-I. Escalante-García, Effect of curing temperature on the nonevaporable water in Portland cement blended with geothermal silica waste, Cement & Concrete Composites 32 (2010) 603–610.
[140] G. Le Saout, E. Lécolier, A. Rivereau, H. Zanni, Chemical structure of cement aged at normal and elevated temperatures and pressures, Part II. Low permeability class G oilwell cement. Cement and Concrete Research 36 (2006) 428–433.
[141] M. Codina, C. Cau-dit-Coumes, P. Le Bescop, J. Verdier, J.P. Ollivier, Design and characterization of low heat and low-alkalinity cements, Cement and Concrete Research 38 (2008) 437–448.
[142] J.I. Escalante-Garcia, J.H. Sharp, The chemical composition and microstructure of hydration products in blended cements, Cement & Concrete Composites 26 (2004) 967–976.
[143] J.L. Garcia Calvo, A. Hidalgo, C. Alonso, L. Fernandez Luco, Development of low-pH cementitious materials for HLRW repositories, Resistance against ground waters aggression. Cement and Concrete Research 40 (8) (2010) 1290–1297.
[144] K. Luke, E. Lachowski, Internal composition of 20-year-old fly ash and slag-blended ordinary Portland cement pastes, Journal of the American Ceramic Society 91 (12) (2008) 4084–4092.
[145] R. Taylor, I.G. Richardson, R.M.D. Brydson, Composition and microstructure of 20-year-old ordinary Portland cement-ground granulated blast-furnace slag blends containing 0 to 100% slag, Cement and Concrete Research 40 (7) (2010) 971–983.
[146] D. Herfort, G. Moir, V. Johansen, F. Sorrentino, H. Bolio Arceo, The chemistry of Portland cement clinker, Advances in Cement Research 22 (4) (2010) 187–194.
[147] H.M. Kanare, E.M. Gartner, Optimum sulfate in Portland cement, *Cements Research Progress 1984*, Am Ceram Soc, Westerville, 1985, p. 213.
[148] E. Gartner, D. Myers, Influence of tertiary alkanolamines on Portland cement hydration, Journal of the American Ceramic Society 76 (1993) 1521–1530.
[149] E. Douglas, G. Pouskouleli, Prediction of compressive strength of mortars made with Portland cement–blast-furnace slag–fly ash blends, Cement and Concrete Research 21 (4) (1991) 523–534.
[150] D. Ravina, P.K. Mehta, Compressive strength of low cement/high fly ash concrete, Cement and Concrete Research 18 (4) (1988) 571–583.
[151] J. Baron, C. Douvre, Technical and economic aspects of the use of limestone filler additions in cement, World Cement 5 (1987) 100–104.
[152] J.S. Damtoft, J. Lukasik, D. Herfort, D. Sorrentino, E. Gartner, Sustainable development and climate change initiatives, Cement and Concrete Research 38 (2008) 115–127.
[153] F.P. Glasser, J. Marchand, E. Samson, Durability of Concrete — Degradation Phenomena Involving Detrimental Reactions, 12th ICCC. Montreal, Canada, 2007, THPL-1.